Ψ_k Newsletter

AB INITIO (FROM ELECTRONIC STRUCTURE) CALCULATION OF COMPLEX PROCESSES IN MATERIALS

Number 99 June 2010

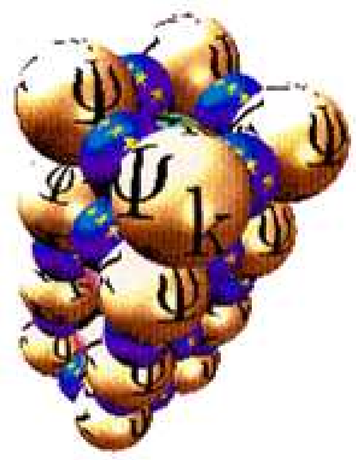

Editor: Z (Dzidka) Szotek
E-mail: psik-coord@dl.ac.uk

Sponsored by: UK's CCP9
and Psi-k

Contents

1 Editorial

We start this newsletter with a brief update on the large Psi-k2010 Conference to be held in Berlin on 12-16 September, 2010. We note that the early/cheap registration for this event has been extended by one week, until Monday, June 7. This information is followed by two workshop announcements and one job announcement. A number of abstracts of newly submitted or recently published papers can be found in the usual section.

The scientific highlight of this issue is on "A Fractional View of the Exchange-Correlation Functional and Derivative Discontinuity in Density Functional Theory" by Aron J. Cohen (Cambridge, UK), Paula Mori-Sánchez (Madrid, Spain) and Weitao Yang (Duke University, USA).

For further details please check the table of content of the newsletter.

The *Uniform Resource Locator* (URL) for the Psi-k webpage is:

`http://www.psi-k.org.uk/`

Please submit all material for the next newsletters to the email address below.

The email address for contacting us and for submitting contributions to the Psi-k newsletters is

	function
psik-coord@dl.ac.uk	**messages to the coordinators, editor & newsletter**

Dzidka Szotek, Martin Lüders and Walter Temmerman
e-mail: psik-coord@dl.ac.uk

2 Psi-k Activities

”Towards Atomistic Materials Design”

2.1 Update on the Psi-k2010 Conference

12-16 September, 2010

Henry Ford Building, Berlin, Germany

Conference Web Page:
`http://www.fhi-berlin.mpg.de/th/Meetings/psik_2010/`

Conference Chair: Matthias Scheffler
Co-Chair: Hardy Gross
Honorary Chair: Volker Heine

The deadline for early registration extended to Monday, June 7!

This is just to update you on the forthcoming Psi-k2010 Conference.

The conference has so far received more than 900 abstracts. This is more than twice as many as at the previous conference which took place in 2005 in Schwäbisch Gmünde, Germany. If you want to be part of this event and have so far forgotten to register please note that the deadline for cheap registration has been extended by a week until June 7.

The five plenary talks of the conference will be given by

Stefano Baroni (Trieste)
Gerbrand Ceder (Boston)
Jens Norskov (Lyngby)
Mark Ratner (Evanston)
David Vanderbilt (Piscataway).

The conference will have 21 symposia and about 110 invited speakers. For details please check the conference web page above.

2.2 Workshop Announcements

2.2.1 CECAM Joint Workshop on Empirical Methods in Semiconductor Nano-Structure Design and Modelling

University College Dublin (Ireland) and University of Manchester (UK)

21-22 June and 23-25 June

CECAM, SFI, STFC Daresbury CECAM node, IoP, ACAM

Stanko Tomić, Eoin P. O'Reilly, Max Migliorato, and Gyaneshwar Srivastava

http://www.cecam.org/workshop-470.html

Two closely coupled CECAM Workshops on the use of empirical methods for semiconductor nanostructure design and modelling will be held in Dublin and Manchester. The first ACAM Workshop (Dublin) focuses primarily on computational/technical issues, numerical implementations and parametrisation strategies, followed immediately by the second STFC Daresbury Workshop (Manchester) highlighting the scientific issues and demands related to empirical nanostructure design and modelling.

A variety of modelling implementations [$\mathbf{k}\cdot\mathbf{p}$, tight-binding, valence force field, empirical pseudopotential, etc.] are being employed that exploit not just the accumulated knowledge of existing experimental and $ab-initio$ results, but also exploit the increased computational power and advanced computational methods now available. The development of empirical methods inherently facilitates synergy between experiment and theory. Proper implementations of empirical methods are capable of delivering new levels of understanding and design for both materials and devices alike. Applications of such schemes span from designing emitters and absorbers used in conventional optoelectronics, through new architectures proposed in quantum information processing, to investigation of novel concepts for the design of future high efficiency solar cells. The workshops address all of these topics and are of relevance both to theoretical and experimental researchers.

Speakers include: Guy Allan, Frederic Aniel, Urs Aeberhard, Gabriel Bester, David Binks, Stefan Birner, Timothy Boykin, Marco Califano, Aldo Di Carlo, Ned Ekins-Daukes, Michael Flatte, Brad Foreman, Guido Goldoni, Pawel Hawrylak, Juan Manuel Llorens Montolio, Mikhail Nestoklon, Andrei Schliwa, Andy Sunderland, Christof Voemel, Lok Lew Yan Voon, Lin-Wang Wang, Bernd Witzigmann, Wlodek Zawadzki, Vladimir Falko.

More information about the workshops and how to register can be found here:
http://www.cecam.org/workshop-470.html

2.2.2 Hands-on SPR-KKR Workshop 2010

October 4-6, 2010

Daresbury Laboratory, United Kingdom

Organized by
H. Ebert and Z. (Dzidka) Szotek

Sponsored by
Daresbury Laboratory Hartree Centre

First Announcement

Interested, contact psik-coord@dl.ac.uk

We are planning to organize a hands-on course where the use of the Munich SPR-KKR code will be taught. The aim of the workshop is to introduce theoreticians as well as experimentalists into the KKR bandstructure method and its use to calculate spectroscopic properties of magnetic solids. Accordingly, there will be lectures dealing with the formal background and technical details of the KKR method. Emphasis will be put on a fully relativistic formulation supplying the basis for a treatment of dichroic effects in spectroscopy. The corresponding theory for magnetic dichroism in x-ray absorption, photoemission and related spectroscopies will be reviewed. Six sessions will be devoted to applications making use of the Munich SPR-KKR program package that include a graphical user interface called Xband. The various calculations on clusters and ordered as well as disordered solids, which are meant in particular to introduce inexperienced users to the field, will be guided by tutors.

There exists a demand from theoreticians and experimentalists alike to be taught the Munich SPR-KKR program. In the past three of these courses took place in Munich, two in Poznan and one at the ALS in Chicago. The format of the course includes six lectures and six computer sessions over an intense three day period. Six lectures will introduce DFT, band theory, the KKR, spectroscopies and the code. The six lectures will be given by: Hubert Ebert (Introduction to the code and the use of Xband, the GUI), Walter Temmerman (Phase Shifts and KKR Multiple Scattering Theory), Peter Dederichs (The KKR as a Green's function method), Jan Minar (Photoemission spectroscopies), Diemo Koedderitzsch (magnetic dichroism), Eberhard Engel (Relativistic DFT). We are expecting up to 30 participants and up to seven tutors.

From past experience we are expecting a mix of theoretical and experimental students which makes these tutorials so stimulating since we will have a poster session where the students can present their results. The experimental students are interested in learning to run the code for one of the spectroscopies, the theoretical students are usually interested in systems where relativistic and spin polarization affect matter and this can be for a surface, a random alloy or an impurity.

The purpose of this preliminary announcement is to find out how many people will be interested to participate in the Daresbury workshop to plan accordingly.

Therefore, if you are interested to participate please send an email to

psik-coord@dl.ac.uk

with 'Hands-on SPR-KKR Workshop' in the subject line, as soon as possible.

3 General Job Announcements

Lectureship in Computational Biological Physics

The Scottish Universities Physics Alliance, The University of Edinburgh and the National Physical Laboratory, U. K.

The Scottish Universities Physics Alliance, The University of Edinburgh and the National Physical Laboratory are seeking to recruit a lecturer at the physics/life sciences interface. This programme arises from the recent growth in the SUPA programme including 11M GBP investment in the area of Physics and the Life Sciences (PALS).

Working in partnership, the NPL and the University of Edinburgh have embarked on a major new research initiative to improve our understanding of technologically relevant biomolecules and biophysical systems across multiple lengthscales enabled by advances in instrumentation and the emergence of new computer architecture. The appointment is jointly funded by NPL and SUPA and for the first four years the successful applicant will spend up to 50their time at NPL in Teddington or engaged in collaborative activities.

The School of Physics and Astronomy is looking to appoint a PALS Lecturer with a track record in advanced computational simulations who will lead the development of an innovative research programme at the life science interface. We are looking for dynamic individuals to develop and/or complement our existing activities. The School has strengths in experimental molecular biophysics, the physics of bacteria, state-of-the-art spectroscopic methods, advanced computational simulations, and ecosystem modelling. You will have prior experience in computational simulation of biologically relevant systems.

Lectureship candidates must provide evidence of peer-reviewed publications and the potential to establish a research programme capable of attracting external funding and will be expected to contribute to teaching.

Prof. Graeme Ackland FRSE
Head of Institute for Condensed Matter and Complex Systems
School of Physics
http://homepages.ed.ac.uk/graeme
Complexity research: www.ph.ed.ac.uk/nania

Secretary: Misti Cooper
Email: misti.cooper@ed.ac.uk
Tel.: +44 (0)131-650-5267

The University of Edinburgh is a charitable body, registered in Scotland, with registration number SC005336.

4 Abstracts

The kaolinite (001) polar basal plane

Xiao-Liang Hu
London Centre for Nanotechnology and Department of Chemistry,
University College London, London WC1E 6BT, U.K.
Angelos Michaelides
London Centre for Nanotechnology and Department of Chemistry,
University College London, London WC1E 6BT, U.K.

Abstract

Kaolinite is thought to be an efficient ice nucleating agent because kaolinite crystals expose perfect unreconstructed (0 0 1) basal surfaces which provide a suitable template for ice growth. However, we show here with the aid of density functional theory calculations that the unreconstructed basal surface is polar. Various mechanisms to eliminate the macroscopic dipole and in so-doing stabilize the basal surface are considered. The most promising option identified so far involves the adsorption of foreign atoms (for example, Na and Cl atoms) on the perfect basal surface, since this yields a non-metallic surface with a cleavage energy lower than the unreconstructed polar basal surface. A quantitative experimental structure determination of the kaolinite basal surface is called for.

(Surface Science **604**, 111 (2010))
Contact person: angelos.michaelides@ucl.ac.uk

A critical assessment of theoretical methods for finding reaction pathways and transition states of surface processes

Jiří Klimeš
London Centre for Nanotechnology and Department of Chemistry,
University College London, London WC1E 6BT, U.K.
David R. Bowler
London Centre for Nanotechnology and Department of Physics and Astronomy,
University College London, London WC1E 6BT, U.K.
Angelos Michaelides
London Centre for Nanotechnology and Department of Chemistry,
University College London, London WC1E 6BT, U.K.

Abstract

The performance of a variety of techniques for locating transition states on potential energy surfaces is evaluated within the density functional theory framework. Diffusion of a water molecule across NaCl(001) and HCl bond breaking on the same surface are treated as general test cases; the former is an example of a low barrier diffusion process and the latter an example of a relatively high barrier covalent bond rupture event. The methods considered include the nudged elastic band (NEB), Dewar, Healy and Stewart (DHS), dimer, constrained optimization (CO), activationrelaxation technique (ART) and one-side growing string (OGS) as well as novel combinations of the DHS with growing string (DHS + GS) and DHS plus climbing image (CI-DHS). A key conclusion to come from this study is that the NEB method is relatively fast, especially when just a single (climbing) image is used. Indeed, using more images represents an unnecessary computational burden for our set of processes. The dimer method exhibits variable performance; being poor for the water diffusion processes, which have small activation energies, but much more efficient for the HCl bond breaking process which has a higher barrier. When only a poor initial guess of the transition state geometry is available, the CI-DHS scheme is one of the most efficient techniques considered. And as a means to quickly establish an approximate minimum energy pathway the DHS + GS scheme offers some potential.

(J. Phys.: Cond. Matt. **22**, 074203 (2010))
Contact person: angelos.michaelides@ucl.ac.uk

Surface energy and surface proton order of the ice Ih basal and prism surfaces

Ding Pan
Institute of Physics, Chinese Academy of Sciences, PO Box 603, Beijing 100190, People's Republic of China
London Centre for Nanotechnology and Department of Chemistry, University College London, London WC1E 6BT, U.K.
Li-Min Liu
London Centre for Nanotechnology and Department of Physics and Astronomy, University College London, London WC1E 6BT, U.K.
Department of Chemistry, University College London, London WC1H 0AJ, UK
Gareth A Tribello
Department of Chemistry, University College London, London WC1H 0AJ, UK
Davy Faraday Research Laboratory, University College London, Kathleen Lonsdale Building, Gower Street, LondonWC1E 6BT, UK
Ben Slater
Department of Chemistry, University College London, London WC1H 0AJ, UK
Davy Faraday Research Laboratory, University College London, Kathleen Lonsdale Building, Gower Street, LondonWC1E 6BT, UK
London Centre for Nanotechnology and Department of Chemistry, University College London, London WC1E 6BT, U.K.
Angelos Michaelides
London Centre for Nanotechnology and Department of Physics and Astronomy, University College London, London WC1E 6BT, U.K.
Department of Chemistry, University College London, London WC1H 0AJ, UK
Enge Wang
Institute of Physics, Chinese Academy of Sciences, PO Box 603, Beijing 100190, People's Republic of China

Abstract

Density-functional theory (DFT) is used to examine the basal and prism surfaces of ice Ih. Similar surface energies are obtained for the two surfaces; however, in each case a strong dependence of the surface energy on surface proton order is identified. This dependence, which can be as much as 50% of the absolute surface energy, is significantly larger than the bulk dependence (¡1%) on proton order, suggesting that the thermodynamic ground state of the ice surface will remain proton ordered well above the bulk orderdisorder temperature of about 72 K. On the basal surface this suggestion is supported by Monte Carlo simulations with an empirical potential and solution of a 2D Ising model with nearest neighbor interactions taken from DFT. Order parameters that define the surface energy of each surface in terms of nearest neighbor interactions between dangling OH bonds (those which point out of the surface into vacuum) have been identified and are discussed. Overall, these results suggest that proton orderdisorder effects have a profound impact on the stability of ice surfaces and will most likely have an effect on ice surface reactivity as well as ice crystal growth and morphology.

(J. Phys.: Cond. Matt. **22**, 074209 (2010))

Contact person: angelos.michaelides@ucl.ac.uk

Proton transfer in adsorbed water dimers

Xiao-Liang Hu
London Centre for Nanotechnology and Department of Chemistry,
University College London, London WC1E 6BT, U.K.
Angelos Michaelides
London Centre for Nanotechnology and Department of Chemistry,
University College London, London WC1E 6BT, U.K.

Abstract

Density functional theory simulations of water on MgO(001) reveal rapid proton transfer within clusters of just two water molecules. Facile dissociation and recombination of the molecules within the dimers along with a concerted surface-mediated exchange of protons between water and hydroxyl molecules makes this possible. We suggest that surface-mediated proton transfer is in general likely to lead to proton transfer in interfacial water systems whenever the relative energies of intact and dissociated states of water are similar.

(To appear on Physical Chemistry Chemical Physics)

Contact person: angelos.michaelides@ucl.ac.uk

The dynamics of quantum tunneling: effects on the rate and transition path of OH on Cu(110)

Erlend Davidson
London Centre for Nanotechnology and Department of Chemistry,
University College London, London WC1E 6BT, U.K.
Ali Alavi
Department of Chemistry, University of Cambridge, Lensfield Road,
Cambridge CB2 1EW, U.K.
Angelos Michaelides
London Centre for Nanotechnology and Department of Chemistry,
University College London, London WC1E 6BT, U.K.

Abstract

Recent low temperature scanning-tunneling microscopy experiments [T. Kumagai et al. Phys. Rev. B. 79, 035423 (2009)] observed the possible quantum tunneling of hydroxyl groups between two equivalent adsorption configurations on Cu(110). Here we analyse the quantum nuclear tunneling dynamics of hydroxyl on Cu(110) using density functional theory based techniques. We calculate classical, semi-classical and quantum mechanical transition rates for the flipping of OH between two degenerate energy minima. The classical transition rate is essentially zero at the temperatures used in experiment, and the tunneling rate along the minimum energy path is also much too low compared to experimental observations. When tunneling is taken into account along a direct path connecting the initial and final states with only a minimum amount of the oxygen movement the transition rate obtained is in much better agreement with experiment, suggesting quantum tunneling effects cause a deviation of the reaction coordinate from the classical transition path.

(To appear on Physical Review B)

Contact person: angelos.michaelides@ucl.ac.uk

Ab initio study of hydrogen insertion in ultra-thin transition metal doped V films. Structural and electronic properties

A. Lebon
Laboratoire de Magnétisme de Bretagne, FRE CNRS 3137
Université de Bretagne Occidentale, 6 avenue Victor Le Gorgeu,
29285 Brest Cedex, France
A. Vega
Laboratoire de Magnétisme de Bretagne, FRE CNRS 3137
Université de Bretagne Occidentale, 6 avenue Victor Le Gorgeu,
29285 Brest Cedex, France
A. Mokrani
Institut des Matériaux Jean Rouxel, UMR CNRS 6502, Université de Nantes,
2 rue de la Houssinière, B.P. 44322 Nantes, France

Abstract

We investigate the insertion of hydrogen in ultra-thin V films with three monolayers in which we consider a substitutional doping impurity of Ca, Sc, Ti, V, Cr, Mn, and Fe. Calculations are conducted within the Density Functional Theory, as implemented in the SIESTA code, to analyze the impact of the different doping impurities on the structural shape and in particular on the different local environments available for hydrogen insertion, as well as on the electronic structure. The impurities located on the left side of vanadium in the periodic table induce a volume expansion in their neighborhood while elements located on the right side induce a contraction. The embedding energy of the H atom indicates that the impurities at the left act as trapping centers. In general, H prefers tetrahedral interstitial sites in the presence of substitutional impurities at the left of vanadium, whereas octahedral interstitial sites are favored when the substitutional element is at the right. In addition, an increase of the density of states is obtained at the Fermi level when H sits on a tetrahedral site. This H effect can be related with experimental observations of transport properties. Finally, a bonding state is obtained at an energy position that depends on both the substitutional impurity and the symmetry of the interstitial site.

(Physical Review B 81, 094110 (2010))

Contact person: A. Lebon (Alexandre.Lebon@univ-brest.fr)

A microkinetic model of ammonia decomposition on a Pt overlayer on Au(111)

K. Rasim[1,2], M. Bobeth[1], W. Pompe[1], N. Seriani[3,4]
[1]*Institute for Materials Science and Max Bergmann Center of Biomaterials, Technische Universität Dresden, 01062 Dresden, Germany*
[2]*Institut des Materiaux Jean Rouxel (IMN), 2 rue de la Houssiniere, 44322 Nantes cedex 3, France.*
[3]*Fakultät für Physik, University of Vienna, Sensengasse 8, A-1090 Wien, Austria*
[4] *The Abdus Salam ICTP, Strada Costiera 11, 34151 Trieste, Italy*

Abstract

Ammonia decomposition is important for a series of technological applications. For developing efficient catalysts for this reaction, basic understanding of underlying mechanisms is fundamental. We have investigated ammonia decomposition on platinum (111) and (100) surfaces, and on a platinum overlayer on a (111) gold substrate within a microkinetic model. The kinetic parameters in the corresponding rate equations have been estimated on the basis of ab-initio calculations of reaction and activation energies for the adsorption and dehydrogenation processes on the catalyst surface. Steady-state coverages of species participating in the decomposition have been determined as solution of the rate equations in the limiting case of small ammonia concentrations of an N_2-NH_3 model gas mixture under flow conditions. Calculated turnover frequencies of ammonia decomposition as a function of the temperature reproduce characteristic features reported for platinum wires. The highest turnover frequency and hydrogen coverage have been obtained for the platinum overlayer on gold. Potential application of this system as ammonia-sensing device is discussed.

Journal of Molecular Catalysis A: Chemical, accepted
Contact person: Karsten Rasim, Karsten.Rasim@cnrs-imn.fr

Structural and magnetic properties of $X_{12}Y$ (X, Y = Fe, Co, Ni, Ru, Rh, Pd and Pt) nanoalloys

F. Aguilera-Granja
Instituto de Física "Manuel Sandoval Vallarta",
Universidad Autónoma de San Luis Potosí,
78000 San Luis Potosí, México

R. C. Longo
Departamento de Física de la Materia Condensada, Facultad de Física,
Universidad de Santiago de Compostela, E-15782 Santiago de Compostela, Spain

L. J. Gallego
Departamento de Física de la Materia Condensada, Facultad de Física,
Universidad de Santiago de Compostela, E-15782 Santiago de Compostela, Spain

A. Vega
Departamento de Física Teórica, Atómica y Óptica, Universidad de Valladolid,
E-47011 Valladolid, Spain

Abstract

We perform extensive *ab initio* density-functional calculations to investigate the structures and magnetic moments of the binary clusters $X_{12}Y$ (X, Y = Fe, Co, Ni, Ru, Rh, Pd, Pt). Although all the binary clusters $Fe_{12}Y$, $Co_{12}Y$, $Ru_{12}Y$ and $Rh_{12}Y$, plus $Ni_{12}Y$ (Y = Rh, Pd, Pt) and $Pt_{12}Y$ (Y = Ru, Rh, Pd), retain, with more or less distortions, the structures of the corresponding pure X_{13} clusters, the remaining binary clusters (i.e., a significant number of 12 of all the 42 cases) adopt geometries different from those of the corresponding pure clusters. Independent of the peculiarities of each family of binary clusters, the binding energies of all the binary clusters $X_{12}Ru$ are bigger than those of the pure X_{13} clusters, while the binding energies of all the binary clusters $X_{12}Pd$ are smaller. The clusters investigated exhibit a variety of magnetic behaviors. In the case of $Ni_{12}Rh$, we predict a remarkable magnetic cooperative phenomenon that can be attributed to electronic effects associated to the chemical environment through Ni-Rh hybridization.

(The Journal of Chemical Physics 132, 184507 (2010))

Contact person: F. Aguilera-Granja faustino@dec1.ifisica.uaslp.mx

Structural Investigation of the (010) surface of the orthorhombic T-Al_3(Mn, Pd) crystal

T. Deniozou[a], R. Addou[a], A. Shukla[a], M. Heggen[b], M. Feuerbacher[b],
M. Krajčí[c,d], J. Hafner[d], R. Widmer[e], O. Groening[e],
V. Fournée[a], J.-M. Dubois[a], and J. Ledieu[a]
[a] *Institut Jean Lamour (UMR7198 CNRS-Nancy-Université-UPVM),*
Ecole des Mines, Parc de Saurupt, 54042 Nancy Cedex, France
[b] *Institut für Festkörperforschung, Forschungszentrum Jülich,*
52425 Jülich, Germany
[c] *Institute of Physics, Slovak Academy of Sciences,*
Dúbravská cesta 9, SK-84511 Bratislava, Slovak Republic
[d] *Fakultät für Physik and Center for Computational Materials Science,*
Universität Wien, Sensengasse 8/12, A-1090 Wien, Austria
[e] *EMPA, Nanotech @ Surfaces, Feuerwerkerstraße 39,*
CH-3602 Thun, Switzerland

Abstract

The atomic structure of the (010) surface of the T-Al_3(Mn, Pd) complex metallic alloy is investigated by means of low-energy electron diffraction (LEED), scanning tunneling spectroscopy (STM), x-ray and ultraviolet photoelectron spectroscopy (XPS, UPS) , x-ray photoelectron diffraction (XPD) and *ab initio* calculations. While structural imperfections are observed at the surface and out of the various possible terminations, the puckered P2 layer is identified as the only surface termination. The measured step heights correspond to distances between identical planes along the [010] direction in the bulk model, i.e b/2. A bias dependency of the STM topography is found. The XPD and LEED patterns confirm the pseudo-10-fold symmetry of the sample. XPS and UPS show a more metallic signature of the T-phase compared to quasicrystalline phases.

(Phys. Rev. B **81** 125418 (2010))
Contact person: fyzikraj@savba.sk

Magnetic coupling parameters at an oxide-oxide interface from first principles: Fe_2O_3-$FeTiO_3$

Hasan Sadat Nabi[1], Richard J. Harrison[2] and Rossitza Pentcheva[1]
[1] *Department of Earth and Environmental Sciences,*
University of Munich, Theresienstr. 41, 80333 Munich, Germany
[2] *Department of Earth Sciences, University of Cambridge,*
Downing Street, Cambridge CB2 3EQ, United Kingdom

Abstract

Charge mismatch at the interface between canted antiferromagnetic hematite (α-Fe_2O_3) and antiferromagnetic ilmenite ($FeTiO_3$) is accommodated by the formation of mixed Fe^{2+} and Fe^{3+} contact layers, leading to uncompensated magnetic moments in the system. To derive the magnetic exchange interaction parameters of the end members and interface we map total energy differences of collinear spin-arrangements obtained from density functional theory calculations to a Heisenberg Hamiltonian using the least-squares method. Parameters for the end members, hematite ($J_m^{3+,3+}$) and ilmenite ($J_m^{2+,2+}$) are in good agreement with the values obtained from inelastic neutron scattering data. The magnetic interaction parameters between Fe^{2+} and Fe^{3+} ($J_m^{2+,3+}$) in the contact layer show a strong antiferromagnetic coupling to the adjacent hematite layers and thus explain the ferrimagnetism in the system.

(Accepted in Phys. Rev. B)

Contact person: hasan.sadat@lrz.uni-muenchen.de

Parallel electron-hole bilayer conductivity from electronic interface reconstruction

R. Pentcheva[a], M. Huijben[b], K. Otte[a], W.E. Pickett[c], J.E. Kleibeuker[b],
J. Huijben[b], H. Boschker[b], D. Kockmann[b], W. Siemons[d], H.J.W. Zandvliet[b],
G. Rijnders[b], D.H.A. Blank[b], H. Hilgenkamp[b], A. Brinkman[b]
[a]*Department of Earth and Environmental Sciences, University of Munich, Germany*
[b]*Faculty of Science and Technology and MESA$^+$ Institute for Nanotechnology, University of Twente, The Netherlands*
[c]*Department of Physics, University of California, Davis, USA*
[d]*Department of Physics, University of California, Berkeley, USA*

Abstract

The perovskite $SrTiO_3$-$LaAlO_3$ structure has advanced to a model system to investigate the rich electronic phenomena arising at polar interfaces. Using first principles calculations and transport measurements we demonstrate that an additional $SrTiO_3$ capping layer prevents atomic reconstruction at the $LaAlO_3$ surface and triggers the electronic reconstruction at a significantly lower $LaAlO_3$ film thickness than for the uncapped systems. Combined theoretical and experimental evidence (from magnetotransport and ultraviolet photoelectron spectroscopy) suggests two spatially separated sheets with electron and hole carriers, that are as close as 1 nm.

(Published in Phys. Rev. Lett. **104**, 166804 (2010).)

Contact person: Rossitza.Pentcheva@lrz.uni-muenchen.de

Coverage dependent adsorption mode of water on $Fe_3O_4(001)$: Insights from First Principles calculations

Narasimham Mulakaluri[1,2], Rossitza Pentcheva[1], Matthias Scheffler[2]
[1]*Dept. of Earth and Environmental Sciences,*
University of Munich, Theresienstr. 41, 80333 Munich, Germany
[2]*Fritz-Haber-Institut der Max-Planck-Gesellschaft,*
Faradayweg 4-6, D-14195 Berlin, Germany

Abstract

Using density functional theory calculations together with an on-site Coulomb repulsion term (GGA+U), we investigate the adsorption of water on $Fe_3O_4(001)$. Starting from a single water molecule per $(\sqrt{2} \times \sqrt{2})R45^\circ$-unit cell, we vary the concentration and configuration of water and hydroxyl groups. Isolated water molecules on the clean surface tend to dissociate heterolytically with an OH-group adsorbed on top of an octahedral iron and a proton donated to a surface oxygen. Furthermore, oxygen defects are found to promote strongly water dissociation. The released protons bind to distant surface oxygen to minimize the repulsive interaction between the surface OH groups. At higher coverages, the interplay between adsorbate-adsorbate and adsorbate-substrate interactions and the formation of hydrogen bonds between the surface species results in a crossover to a mixed adsorption mode where every second molecule is dissociated. The energetic trends are related to the underlying electronic mechanisms.

(Accepted in J. Phy. Chem. C, May (2010))
Contact persons: Rossitza.Pentcheva@lrz.uni-muenchen.de,
or mulakaluri.narasimham@lrz.uni-muenchen.de

Secondary structure of Ac-Ala$_n$-LysH$^+$ polyalanine peptides (n=5,10,15) in vacuo: Helical or not?

M. Rossi[1], V. Blum[1], G. von Helden[1], F. Bierau[1], K. Pagel[2,3], G.Meijer[1],
and M. Scheffler[1]
[1] *Fritz-Haber-Institut der Max-Planck-Gesellschaft,*
Faradayweg 4-6, 14195 Berlin, Germany
[2] *Freie Universität Berlin, Institut für Chemie*
und Biochemie, D-14195 Berlin, Germany
[3] *University of Oxford, Chemistry Research Laboratory,*
Mansfield Road, Oxford OX1 3TA, UK

Abstract

The polyalanine-based peptide series Ac-Ala$_n$-LysH$^+$ (n=5-20) is a prime example that a secondary structure motif which is well-known from the solution phase (here: helices) can be formed *in vacuo*. We here revisit this conclusion for n=5,10,15, using density-functional theory (van der Waals corrected generalized gradient approximation), and gas-phase infrared vibrational spectroscopy. For the longer molecules (n=10,15) α-helical models provide good qualitative agreement (theory vs. experiment) already in the harmonic approximation. For n=5, the lowest energy conformer is not a simple helix, but competes closely with α-helical motifs at 300 K. Close agreement between infrared spectra from experiment and ab initio molecular dynamics (including anharmonic effects) supports our findings.

(Submitted to: J. Phys. Chem. Lett.)

Contact person: Mariana Rossi (rossi@fhi-berlin.mpg.de)

Large-scale surface reconstruction energetics of Pt(100) and Au(100) by all-electron DFT

P. Havu[1,2], V. Blum[1], V. Havu[1,2], P. Rinke[1], and M. Scheffler[1]
[1] *Fritz-Haber-Institut der Max-Planck-Gesellschaft,*
Faradayweg 4-6, 14195 Berlin, Germany
[2] *Aalto University, Department of Applied Physics,*
P.O. Box 11100, FI-00076 AALTO, Finland

Abstract

The large-scale quasihexagonal surface reconstructions of Au(100) and Pt(100) are among the biggest surprises of early surface science. Still, some significant questions regarding their reconstruction energies remain even today (rather dissimilar Au and Pt in the available experiments, and experiment and theory do not match for Pt). We here use density-functional theory in an all-electron implementation and large enough approximant supercells - "(5 x N)", N=10-30 - to show that the reconstruction energies of both surfaces are in fact similar, and closer to the measured value for Pt(100) *in vacuo*. Additionally, our calculations demonstrate excellent agreement with known geometry characteristics of both surfaces and corroborate earlier work that suggested relativistically enhanced d-d hybridization as the driving force of the reconstruction.

(Submitted to: Phys. Rev. Lett.)

Contact person: Paula Havu (havu@fhi-berlin.mpg.de)

Li-doped MgO: Temperature dependent morphology, magnetic and optical properties

Philipp Myrach[1],Niklas Nilius[1], Sergey V. Levchenko[1], Anastasia Gonchar[1],
Thomas Risse[1], Klaus-Peter Dinse[2], Lynn A. Boatner[3],
Wiebke Frandsen[1], Raimund Horn[1], Hans-Joachim Freund[1],
Robert Schlögl[1], Matthias Scheffler[1]
[1]*Fritz-Haber-Institut der Max-Planck-Gesellschaft,*
Faradayweg 4–6, 14195 Berlin, Germany
[2]*Fachbereich Physik, Freie Universität Berlin,*
Arnimallee 14, D–14195 Berlin, Germany
[3]*Solid State Division, Oak Ridge National Laboratory,*
P.O. Box 2008, Oak Ridge, TN 37831

Abstract

Li-doped MgO might be a potential catalyst for the oxidative coupling of methane, whereby surface Li^+O^- centers are suggested to be the chemically active species. To elucidate the role of Li in the MgO matrix, we have prepared two model systems and investigated their morphological, optical and magnetic properties as a function of the Li-doping. The first one is an MgO film deposited on Mo(001) that was doped with various amounts of Li. The second one is a powder sample, being fabricated by calcination of Li and Mg precursors in an oxygen ambience. Scanning tunneling and transition electron microscopy have been performed to characterize the morphology of both samples. At temperatures above 700 K, Li starts segregating towards the surface and forms irregular Li-rich oxide patches. Above 1050 K, the Li desorbs from the MgO support, leaving behind a characteristic defect pattern. Traces of Li also dissolve in the MgO matrix at high temperature, as concluded from a distinct optical signature that is absent in the pristine oxide. No electron-paramagnetic-resonance signal was detected in the explored samples, which would be compatible with the formation of Li^+O^- centers. Furthermore, density-functional-theory calculations have been carried out to determine the thermodynamic stability of possible Li-induced defects in the MgO. The calculations clarified the driving force for the observed Li segregation towards the MgO surface, but also rationalized the absence of Li^+O^- centers. From the combination of experimental and theoretical results, a comprehensive picture of the role of Li on the physical properties of MgO arises, which forms a solid basis to analyze the chemical behavior of the doped oxide material in future.

(ChemCatChem, accepted (18 May, 2010))
Contact person: Sergey Levchenko (levchenko@fhi-berlin.mpg.de)

5 SCIENTIFIC HIGHLIGHT OF THE MONTH: ”A Fractional View of the Exchange-Correlation Functional and Derivative Discontinuity in Density Functional Theory”

A Fractional View of the Exchange-Correlation Functional and Derivative Discontinuity in Density Functional Theory

Aron J. Cohen[1], **Paula Mori-Sánchez**[2] **and Weitao Yang**[3]

[1]Department of Chemistry, Lensfield Rd, University of Cambridge, CB2 1EW, UK
[2]Department of Chemistry, Universidad Autónoma de Madrid, Madrid 28049, Spain
[3]Department of Chemistry, Duke Univeristy, Durham, North Carolina, 27708, USA

Abstract

The exchange-correlation functional is the key object in the understanding and application of density functional theory (DFT). Development of approximations to the exact functional is extremely challenging, as it aims to give a universal functional that works for all densities. To shed light on this issue in any manner is of great importance, and exact conditions offer a possible path forward. By considering the well established formal extension of DFT to fractional occupations at zero-temperature, we formulate perspectives based on fractional numbers of electrons and fractional spins that reveal some very stringent exact conditions of the energy functional. What is possibly even more important is that currently used approximations violate these exact conditions, leading to massive basic errors in very simple molecules and trends in extended systems that explain systematic errors in the electron density, energy and their derivatives from DFT calculations. This is exemplified by the delocalisation error and static correlation error. The further combination of these two concepts leads to understanding of the band-gap and the derivative discontinuity in DFT, sheds light on the calculation of strongly correlated systems, and calls for dramatically new functional forms that have a discontinuous nature.

5.1 Introduction

The total energy in density functional theory (DFT) [1–8] is given by

$$E[\rho] = \sum_i^N \langle\phi_i| - \frac{1}{2}\nabla^2|\phi_i\rangle + \int \rho(\mathbf{r})v_{\text{ext}}(\mathbf{r})\mathrm{d}\mathbf{r} + J[\rho] + E_{xc}[\rho] \tag{1}$$

where the non-interacting reference system has N electrons in N orbitals, and electron density

$$\rho(\mathbf{r}) = \sum_i^N |\phi_i(\mathbf{r})|^2. \tag{2}$$

When the orbitals are eigenstates of a local potential, the reference system is the original Kohn-Sham system [9]. When the orbitals are eigenstates of a nonlocal potential, the reference system is the generalised Kohn-Sham system [10]. The key to the success of DFT is that simple approximations for the exchange-correlation functional perform remarkably well for a wide range of problems and are extremely accurate for large areas of chemistry and physics, particularly for prediction of the structures and thermodynamic properties of molecules and solids. In particular, hybrid [11–13] and screened hybrid functionals [14, 15] have demonstrated significantly improved performance for certain properties such as band structure and band gap prediction, over the local density approximation (LDA) and the generalised gradient approximation (GGA). On the other hand, the range-separated approach with different treatments for the long- and short-range parts of electron-electron Coulomb interaction operator, originally formulated by Savin [16] and early work by Gill [17], has lead to much improved property prediction for charge transfer systems or optical responses by Hirao and coworkers [18, 19] and Handy and coworkers [20]. It also motivated screened-Coulomb functionals with much improved description of band structure of solids by Scuseria and coworkers [15], and functionals by the present authors [21]. Related development has also been made by Baer and Neuhauser [22], based on the generalised adiabatic connection developed by Yang [23].

How do we move forward in the development of the exchange-correlation functional? Will the inclusion of more and more parameters and complicated ingredients (e.g. exact exchange, using range-separation, modelling the adiabatic connection [24–27], local hybrids [28–31], double hybrids [32–34] or other uses of the unoccupied orbitals and eigenvalues [35–37] etc.) lead to dramatically better functionals? Obviously the more flexible the form in functional space there is the possibility for improvement, but unfortunately no systematic way forward is highlighted. What we want to offer in this review is a perspective on DFT which allows us to understand many of the failures of the above approximations and also offers a path for the development of new and better exchange-correlation functionals. For this we consider a very simple extension of DFT to fractional occupations.

5.2 A fractional perspective

Perdew, Parr, Levy and Balduz (PPLB) in a seminal paper in 1982 [38] extended density functional theory to non-integer numbers of electrons by considering a zero temperature grand-canonical ensemble. They found that for fractional numbers of electrons, $N + \delta$ $(0 \leq \delta \leq 1)$ the exact density and exact energy are given by ensemble averages of the integers either side (N and $N + 1$)

$$\begin{aligned} \rho_{N+\delta}(\mathbf{r}) &= (1-\delta)\rho_N(\mathbf{r}) + \delta\rho_{N+1}(\mathbf{r}) && (3) \\ E_{N+\delta} &= (1-\delta)E_N + \delta E_{N+1} && (4) \end{aligned}$$

as is illustrated in Fig. 1. This is an extremely key result in DFT, both for understanding the theory and also approximate functionals. It can be viewed as an exact condition that functionals should satisfy.

A natural question is why should one care about the behaviour of functionals for fractional charges, which are not physical objects. A good answer is illustrated by the pure state derivation

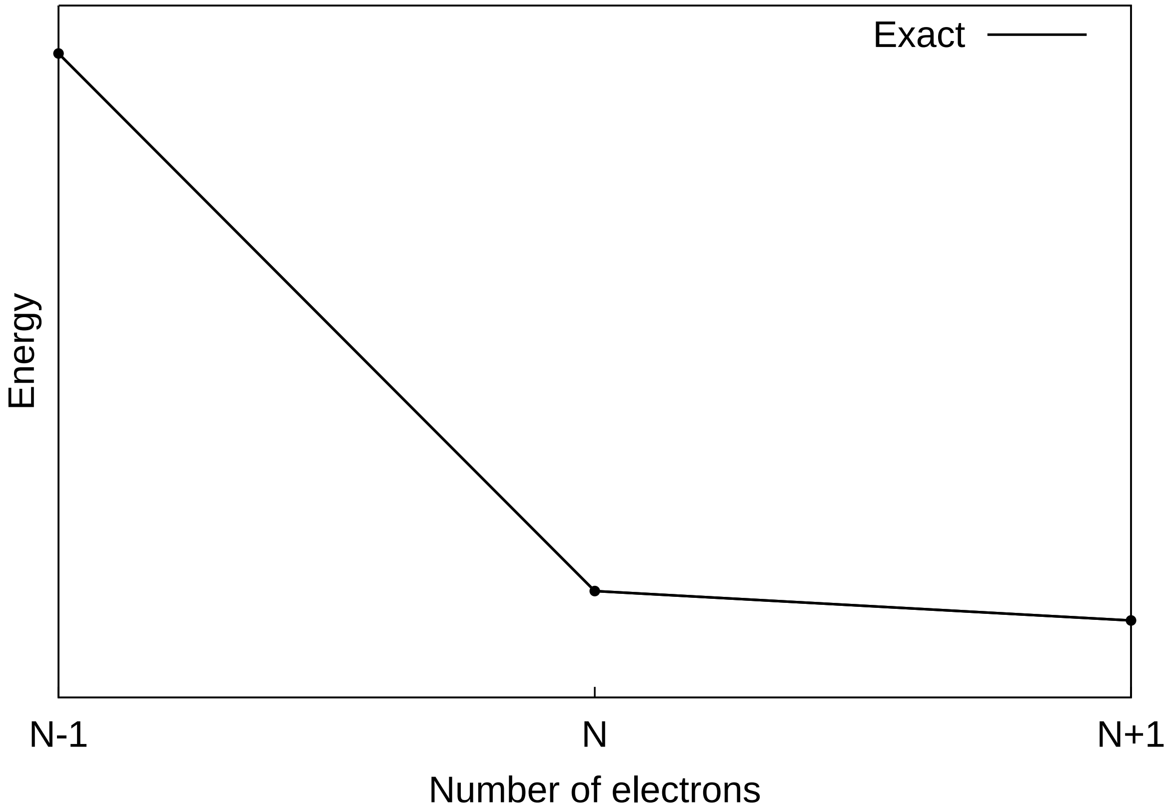

Figure 1: Behaviour of the total energy with respect to the number of electrons. For a fractional charge system, $N+\delta$, the exact energy is a linear interpolation between the N and $N+1$ systems.

of the PPLB result, Eq. (4) [39]. One starts from a pure state of a system and takes the system to the limit of dissociation into identical subsystems. The subsystems have fractional charges and the densities are in ensemble form. Since the energy functional should be size-extensive, this forces the energy functional to be defined for fractional charges. In other words, in order to satisfy the size extensivity requirement, the exact density functional must be defined for ensemble densities with fractional charges. Furthermore, as will be shown, the conditions on the behaviour of the functional for fractional charges are critically important, as their violation is the cause of major failure of approximate functionals.

In Kohn-Sham theory, fractional charges can be treated in a very simple manner [40]. A ground state system where the total number of electrons, N, is now allowed to be non-integer, and has

$$N = \sum_i n_i \tag{5}$$

with occupation numbers

$$n_i = \begin{cases} 1, & i < i_{max} \\ \delta, & i = i_{max} \\ 0, & i > i_{max} \end{cases} \tag{6}$$

density

$$\rho(\mathbf{r}) = \sum_i n_i |\phi_i(\mathbf{r})|^2 \tag{7}$$

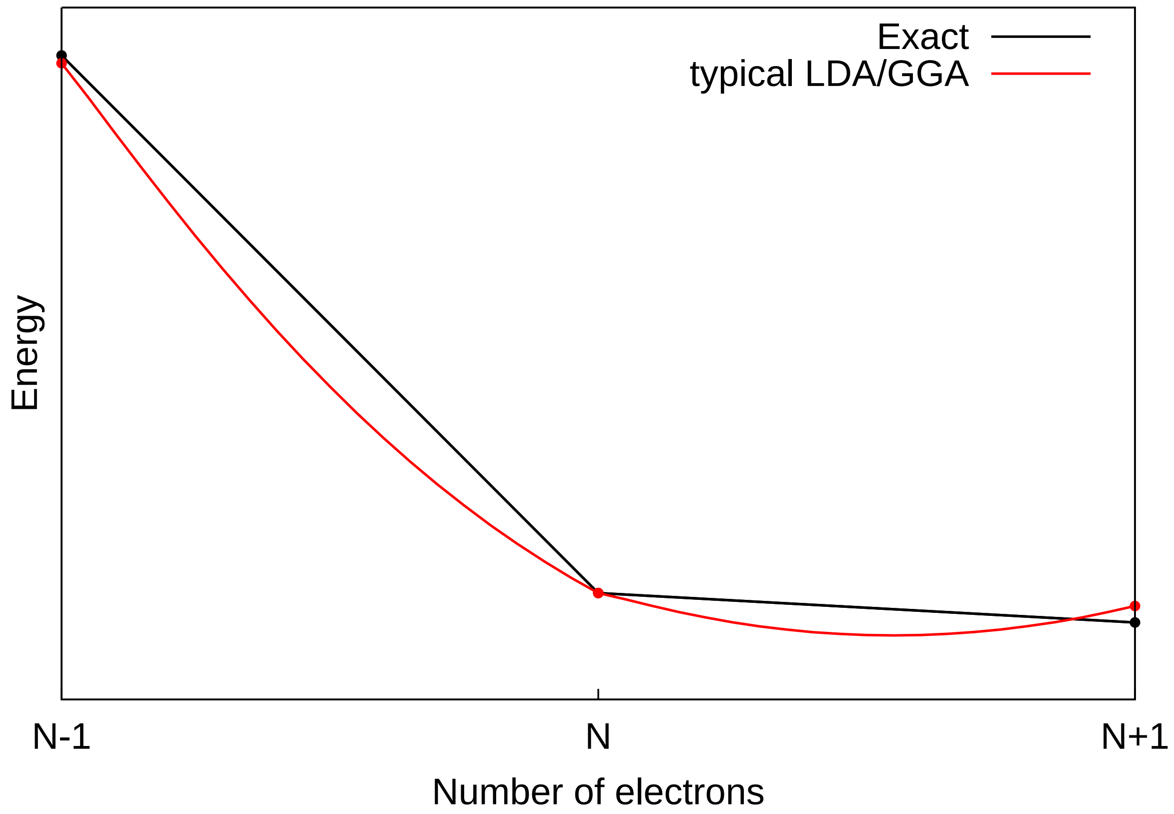

Figure 2: Energy versus number of electrons for the exact functional and the typical incorrect convex performance of LDA or GGA.

and corresponding total energy

$$E[\rho] = \sum_i n_i \langle \phi_i | -\frac{1}{2}\nabla^2 | \phi_i \rangle + \int \rho(\mathbf{r}) v_{\mathrm{ext}}(\mathbf{r}) \mathrm{d}\mathbf{r} + J[\rho] + E_{xc}[\rho]. \tag{8}$$

The behaviour of approximate exchange-correlation functionals for this extension to fractional shows up a key failure, as illustrated in Fig. 2. Typical approximations such as LDA or GGA often give good energies at integer number of electrons (especially for finite systems) but have an incorrect convex behaviour for systems with fractional charges [41–44]. This is a very basic error that affects some of the most simple aspects of practical calculations such as densities, energies and derivatives.

5.2.1 Densities

Consider one of the ways to derive the exact behaviour of the total energy for fractional charges (e.g. systems with non-integer electron number) using ensembles of stretched molecules [39]. Let us consider the simplest molecule, H_2^+, with two protons A and B and let us analyse three possibilities (see Fig. 3): first the electron is on proton A, secondly the electron is on proton B. From the point of view of the density these two look the same and unsurprisingly have the same energy. Thirdly, a simple linear combination of the two pure states is considered, which leads to half an electron on each proton. From the point of view of the wavefunction this is a just a linear combination of two degenerate orthogonal wavefunctions that is also degenerate.

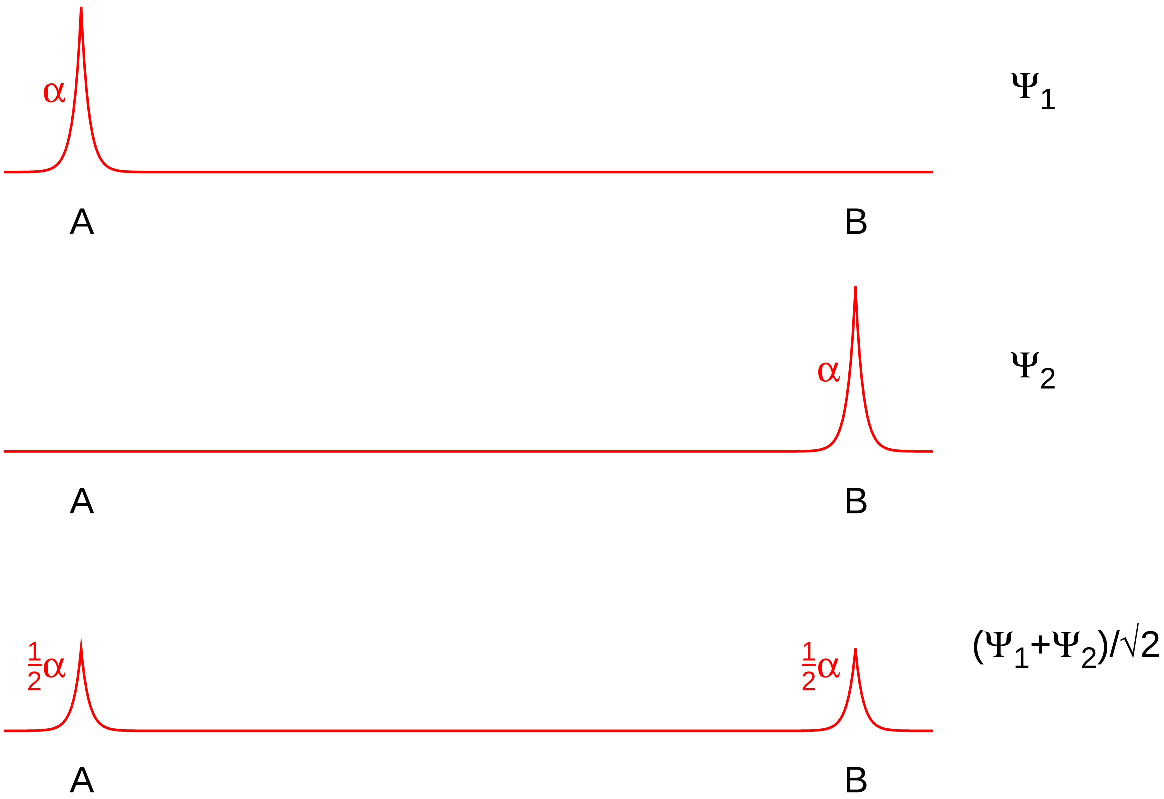

Figure 3: Analysis of H_2^+ at dissociation. The linear combination of pure states with integer occupations (top two) gives rise to a system (bottom) with fractional charges (in this case half an electron) on each proton, and density in an ensemble form.

Nevertheless, from the view of the density, we get a solution that looks very different to the two previous cases and from first consideration it is not clear that it should be degenerate in energy. However, the energy of two protons each with half an electron it is in fact degenerate with the energy of one hydrogen atom, $2E[\mathrm{H}^{1/2+}] = E[\mathrm{H}]$. This illustrates the linearity condition in Eq. (4), that the energy of H with half an electron is halfway in between H with zero electrons and H with one electron.

One idea in the development of functionals is that the exact functional could be found by fitting to every possible chemical species with an infinite number of parameters. So far, functionals have been fitted to approximately a 1000 systems, which cover different areas of chemistry [45–47]. However the space of functionals is massive (much bigger than real space) with all possible densities needed to fully validate approximate functionals. However, the extension to fractional allows us to examine some densities that are very different from the usual ones considered in functional development. We also know exact energies for these densities, as exemplified by the PPLB equation, and very importantly we see massive failures for LDA and GGA.

5.2.2 Energy

The area of DFT is well established, with the foundational theorems proving that the exact exchange-correlation functional exists, and the Kohn-Sham approach and its extensions providing the framework for the implementation of approximate functionals. However, how accurate an approximate functional is, that is how does any particular functional connect to the exact formulation of DFT, is a difficult question to answer and to know *a priori* without testing on certain applications. Here derivation and understanding of exact constraints plays a critical role, especially the ones related to energetics. A very good example is given by the PPLB linearity condition for fractional charges, which is a very stringent test for approximate functionals. While most of the components of the commonly used functionals are not at all linear, e.g., $J[\rho]$ and $E_{xc}^{\mathrm{LDA}}[\rho]$, somehow for density with fractional charges, the exact total energy functional has to be depend linearly on the fractions. As in Zhang and Yang [48], consider the simple homogeneity scaling of the density for between 0 and 1 electrons, $\rho_q = q\rho$. It is very easy to see the scaling of each of the pieces of the energy in Eq. 1: $T_s[\rho_q] = qT_s[\rho]$, $V_{ne}[\rho_q] = qV_{ne}[\rho]$ and $J[\rho_q] = q^2J[\rho]$. Also the exact behaviour of the total energy $E[\rho_q] = qE[\rho]$ is known from the linear behaviour of PPLB. In this very simple case, it is obtained that

$$E_{xc}[\rho_q] = q(1-q)J[\rho] + qE_{xc}[\rho]. \tag{9}$$

This expression shows a key understanding of the errors of exchange-correlation functionals for fractional charges. There are two main parts, a contribution that cancels the quadratic behaviour of the Coulomb term, and a linear exchange-correlation term. For one electron systems, where $E_{xc}[\rho] = -J[\rho]$, this equation could be simplified further into a scaling relation $E_{xc}[\rho_q] = q^2E_{xc}[\rho]$. These important scaling relationships are again violated by functional approximations in the literature.

5.2.3 Derivatives

The E vs N curve and the DFT extension to fractional charges give very important understanding that goes beyond the total energy. This perspective it is in fact key to understand other important concepts, for example, the derivatives of the total energy at a given integer number to the left (electron removal) and to the right (electron addition) give the ionisation energy and election affinity respectively [38, 49, 50],

$$\left.\frac{\partial E}{\partial N}\right|_{N-\epsilon} = -I \qquad \left.\frac{\partial E}{\partial N}\right|_{N+\epsilon} = -A. \tag{10}$$

These are again exact conditions satisfied by the exact E_{xc}. How these are evaluated with a given functional form is an interesting question that again can give insight into the behaviour of approximate functionals. This issue has lead to a great deal of controversy and debate in the literature about the meaning of the eigenvalues and about the role of the derivative discontinuity of the exchange-correlation functional [51–64]. However, this understanding becomes much simpler when viewed from the fractional charge perspective, which can indeed give us a key to some of the failures of currently used approximate functionals as well as guidance for future developments.

From the E vs N picture (Fig. 1) it is clear that the derivatives to the left and the right (at the integer) give I and A and, in principle, and should be obtained by one single calculation at N. Functionals that are not straight lines in between the integers obviously do not give I and A from their derivatives at N.

5.3 Fractional perspective versus classical ensemble view

Let us go back to the consideration of the H_2^+ molecule, stretched to the dissociation limit. Most functional approximations lead to the solution of half an electron on each proton. However, it is important to understand that spreading out the charge is not incorrect in this case, what it is incorrect is just that the energetic favourability for that, e.g. the corresponding unphysical drop in energy.

If the key question was what is the energy of a hydrogen atom with half an electron $H^{\frac{1}{2}+}$, we could just use the exact linearity result from PPLB and take the ensemble average of the energies at 0 electrons and at 1 electron to get a very reasonable result with any functional. However, this is not the question in real applications, where all we get to know is the electron density distribution that, in this case, corresponds to an ensemble density. We are not so interested in that particular fractionally charged system in itself, just in understanding deeper the exact conditions related to this issue and the violation by functional approximations that can lead to important failures in real applications. For this understanding, it is key what type of ensemble is taken (for example the classical ensemble of energies versus an ensemble of densities in our fractional perspective), and it is important to realise that the ensemble must be taken at the level of the basic variable.

Obviously, for the exact functional, the ensemble sums of density and energy are simultaneously true, as in Eqs. (3-4). To examine approximate functionals, we input the ensemble density of Eq. (3) in the approximate functional. The ensemble density is normally represented in terms of ensemble of densities from non-interacting reference systems of N and $N+1$ electrons, which is equivalent to the fractional occupations of one-electron orbitals, Eq. (7). Furthermore, calculations are carried out self-consistently.

All our considerations are not only valid for DFT, but also for many-body methods [65, 66]. In the case of DFT, the basic variable is the noninteracting one particle density matrix, where one uses directly fractional occupations Eq. (6), and in case of many-body methods such as RPA it would be the single particle Green function. Taking ensembles at different levels lead to very different ensemble extensions and help answer very different questions. For understanding failures of methods, the fractional extension performed at the level of the basic variable is key [66].

5.4 Fractional charges and delocalisation error

We have seen how fractional charges emerge in the stretched limit of physical systems. It is very important to understand how considering these systems with fractional charges, which could appear to be quite ficticious, affect real systems in applications. Obviously, it is of key importance to considering frontier orbitals or eigenvalues, analysing band gaps etc. However, the real importance arises in trying to see even more basic problems with density functional approximations. This is clearly illustrated by realising how an incorrect description of fractional charges is deeply related to a more general and fundamental inconsistency of functional approximations, the delocalisation error.

Fig. 4 explains the nature of the delocalisation error [6]. Consider a molecule and an energy

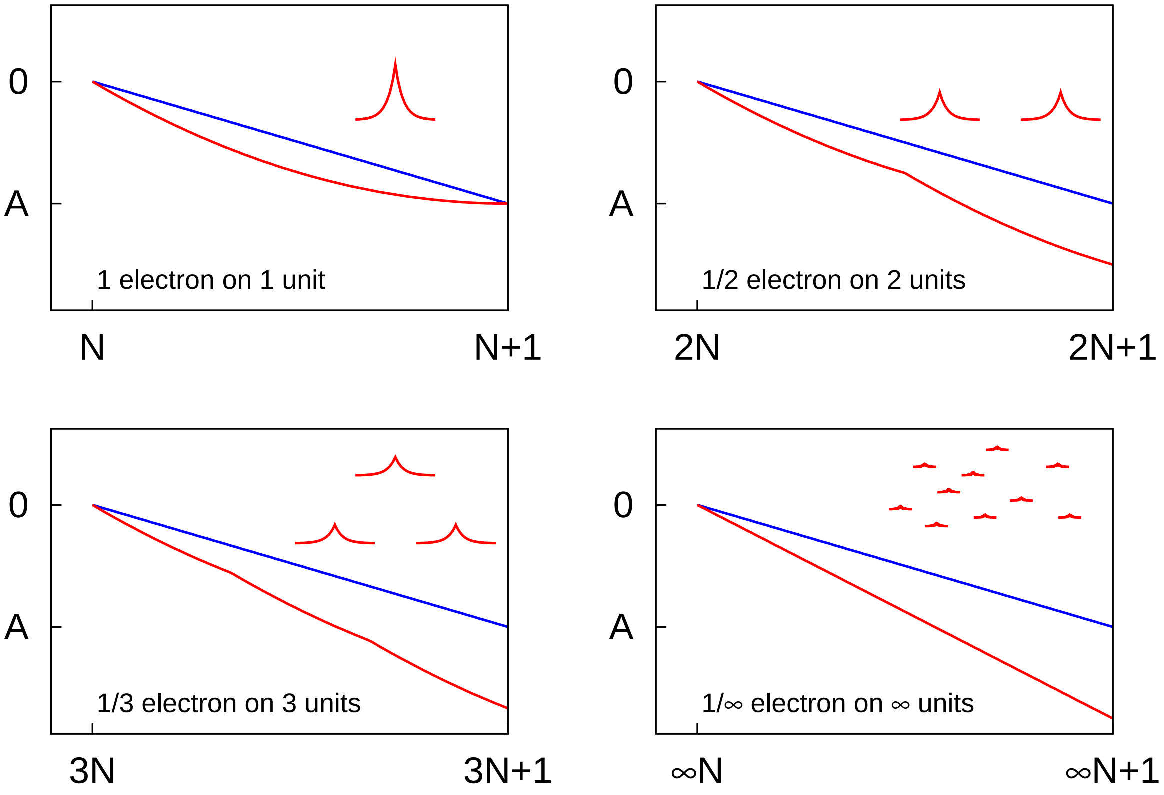

Figure 4: Illustration of the delocalisation error. We plot energy versus number of electrons curves for the addition of up to one electron to a single monomer unit, an infinitely separated dimer, an infinfitely separated trimer and infinitely expanded solid.

functional that has the correct behaviour at the integers N and $N + 1$. The key question is why does it matter that it has incorrect convex behaviour at fractional numbers of electrons in between the integers (as is the typical behaviour for LDA or GGA). Obviously, there is no difference for any calculation on that molecule at integers (the neutral or the negative ion). However, if we now take two of these molecules infinitely separated and consider the neutral and negative ion of that supermolecule, a convex functional will give an incorrect energetic preference for putting half an electron on each monomer. With three molecules the lowest energy would be a third on each with an even lower energy and so on, such that the more molecules separated by infinity the more the functional spreads out the electron and the lower and more unphysical the energy will be (see Fig. 4). In the infinite limit, it is easy to see that this is clearly a wrong solution, as all the possible fractional situations should be degenerate with the electron affinity of the single molecule. However, it is obtained that a convex functional such as LDA in this prototypical case gives a large energetic preference to delocalise the added electron, and also this delocalisation error grows with the size of the system. This argument applies in the infinite limit, but it carries over into non-infinitely separated systems, as it is just showing up the tendency of approximate functionals to spread out charges and the energetic preference for a delocalised density over a localised density. This is a basic problem in DFT, as the electron density distribution should be dictated by the physics of the system, more than intrinsic errors of the functional approximations.

Figure 5: Pictures of diamond and graphite with surfaces of densities corresponding to non-covalent interactions (low density and reduced gradient, see Ref. [67]), represented in green and purple. However, a very interesting question is if approximate functionals that suffer from delocalisation error can predict the sensitive energy differences between the delocalised densities (not pictured) in the aromatic rings of graphite and the cage type localised density of diamond. Even further, it is not clear if they will be able to correctly predict the phase transistion from one to other or they will exhibit quantitative errors, as seen for the isomerisation energies of small molecules.

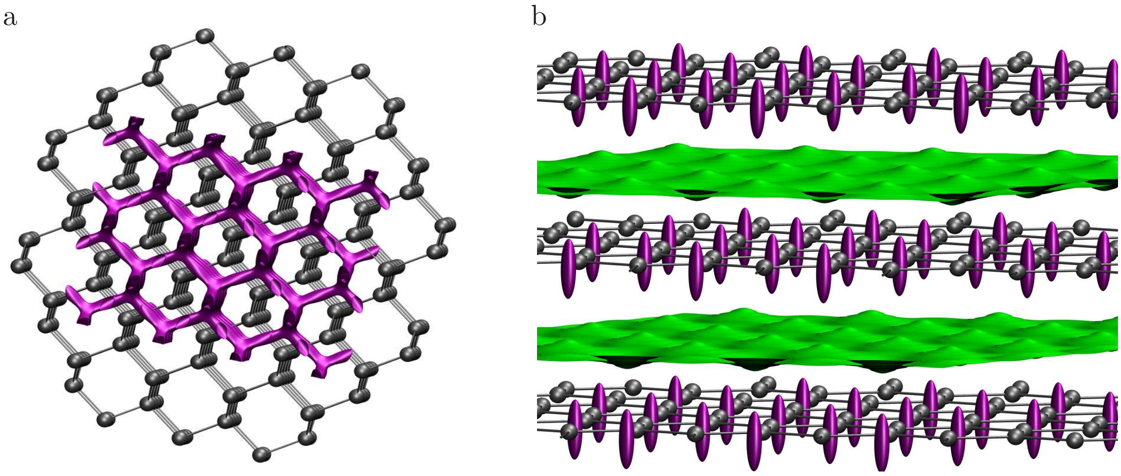

This systematic preference for delocalised densities also effects many other properties. For example with energetics, it carries over to several aspects of organic chemistry. Usually, functional approximations have quite a good performance for many of the energetic differences in organic chemistry, with functionals often designed to reproduce the atomisation energies or heats of formations of small organic molecules [68,69]. One first set of problems have been seen with the prediction of barrier heights of simple chemical reactions, where LDA and GGA give a consistent large under-prediction of the barrier heights [70–72]. There has also been many groups trying to understand some energetic differences for which most functional approximations fail [73–77]. In fact one of the first major problems for DFT was seen in the isomerisation energy of C_{20} [78], with the incorrect ordering of the ring, bowl and cage isomers.

Many other energetic differences can be seen to have an incorrect overstabilisation of delocalised aromatic densities versus the energetics of less delocalised densities [79–81], also related to Fig. 5. Interestingly, the opposite has also been seen in the product of Diels Alder reactions [82]. Here functionals such as BLYP and B3LYP give an incorrect energetic destabilisation of the Diels Alder products. If we analyse a very simple case such as the addition of a ring and C=C double bond to give a small cage [2,2,2] bicyclooctane, BLYP incorrectly underpredicts the heat of formation of the Diels-Alder product by around 20 kcal/mol. This is quite unusual for an organic molecule with just normal C-C bonds, especially to underpredict. One possible answer is that if BLYP has an energetic stabilisation for delocalised densities, then the opposite may be true, such that for a more localised density BLYP may suffer from an energetic destabilisation. This lead us to think that maybe the cage Diels-Alder product had a piece of density that is more ‘localised’ than normal. This argument fitted with the energetics and lead us to look for these pieces of density, which were actually seen in the real space and have been developed into a way to reveal the non-covalent interactions [67]. Whether this delocalisation error argument gives the complete picture is not fully clear, as other GGA functionals such as PBE have a slightly improved performance [83], though still an error of 10 kcal/mol for these systems (even though there convexity for the E vs N curve is very similar). In any case, this analysis in terms of delocalisation error seems to be a useful indication of the power of the E vs N curve and the in depth understanding of the functionals and their results in calculations. There are obviously many other errors that in part have an element of the delocalisation error as their basis.

Overall we believe that the understanding of fractional electrons, once it has been translated into the language of delocalisation, can be very useful to rationalise many of the systematic errors of functionals for many different properties which otherwise seem unconnected. This is key to the further development of functionals free from a bias to artificially localise or delocalise the electrons that improve on properties related to delocalisation error.

5.5 Fractional spins and static-correlation error

There is another set of well known problems in DFT that can be explained, in a related manner to the fractional charge case, by introducing the concept of fractional spins [7]. Again it can be started by considering a simple problem of degeneracies [84, 85]. For stretched H_2 [29, 86–88], see Fig. 6, there are two symmetry broken degenerate wavefunctions, one with an α (spin-up) electron on A and a β (spin-down) electron on B, the second with a β electron on A and an α electron on B. These two are orthogonal and clearly degenerate, both having very similar looking densities. However, the linear combination of these two gives a system that looks very different, two protons each with half an α electron and half a β electron. From the consideration of the wavefunctions that give the densities, it is obviously degenerate. This means that a hydrogen atom with half an α and half a β electron has the same energy as the usual hydrogen atom with one α electron. Again, fractional spin systems are derived by considering pure spin states at dissociation.

More generally the argument above can be formulated as the constancy condition for the exact energy functional, such that systems with any fractional occupation of degenerate spin states should have an energy equal to the integer-spin states as derived in [7, 39],

$$E\left[\sum_{i=1}^{g} C_i \rho_i\right] = E\left[\rho_i\right] = E(N). \tag{11}$$

Approximate functionals have a massive error for these fractional-spin states, giving rise to massive energy overestimations, that explain the errors observed at molecular dissociation. In the typical example of the restricted stretching of H_2, the overestimation of the energy of the fractional spin hydrogen atom exactly matches the error seen at dissociation. In general, the violation of the constancy condition for fractional spins gives to the static correlation error of approximate functionals that is seen throughout applications (e.g. dissociation of molecules, transition metal calculations, etc...)

In quantum chemistry the problems related to static correlation are often thought of as multi-

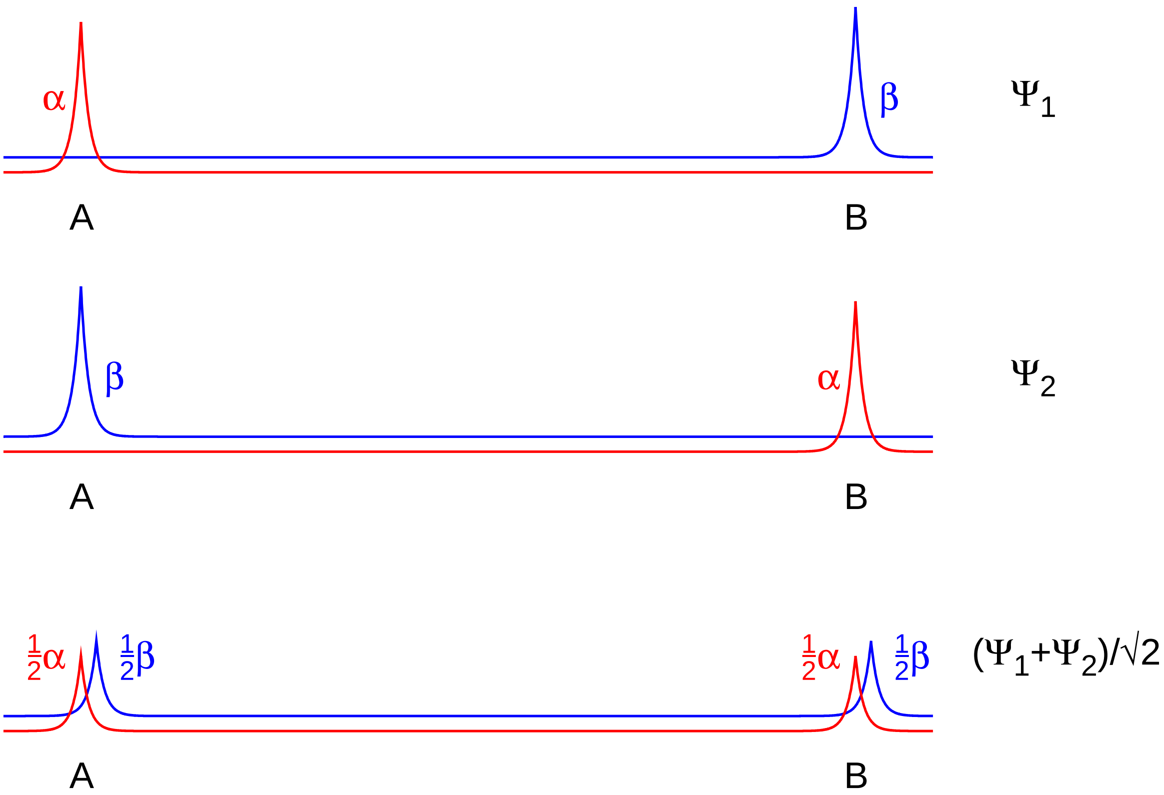

Figure 6: Analysis of H_2 at dissociation. The linear combination of states with integer spin occupations (top two) gives rise to a system (bottom) with fractional spins (in this case half an α electron and half a β electron) on each proton, and density in an ensemble form.

determinantal, where the wavefunction needed cannot be well described by a single determinant [89–91]. However, from the point of view of the density this view does not help much, instead all that is needed are functionals that obey the constancy condition. This again moves the challenge from finding the wavefunction for a particular system to finding better universal exchange-correlation functionals. Again we are testing on a much broader set of densities for which the exact constraints are known. However, this issue poses many open questions. For example, the half β and half α hydrogen atom at the limit of stretched H_2 offers a particular challenge for functionals, especially local ones, as it needs a global view that is able to tell the difference between it and a Helium atom.

All functionals in the literature fail to describe these fractional spin systems, which should be degenerate with the corresponding pure spin states. In this case though the energy is too high, as opposite to the fractional charge case. In the infinite limit, it is possible to obtain the correct energy by breaking the spin symmetry, however it is known (from experiment or full CI calculations) that H_2 has zero spin-density everywhere at any finite distance. The use of symmetry-breaking can be thought of as avoiding the errors of approximate functionals by looking at a state that is slightly incorrect (except in the limiting case). It will often give reasonable numbers for calculated experimental quantities, but should probably not give perfect agreement with experiment in all cases. In fact, this incorrect preference for symmetry breaking in the simple prototypical example of H_2 may explain other related issues, as many of the difficulties in calculation of magnetism in the solid state. It is expected that functionals would generally like to localise the spins and, for example, would have an energetic preference for an antiferromagnetic state over a closed shell diamagnetic one. The errors of the functionals augment as the proportion of exact exchange is increased in the functional, with Hartree-Fock giving a much larger error than LDA or GGA, and with hybrid functionals in between.

5.6 Unified conditions for fractional charges and fractional spins

The fractional charge and fractional spin perspectives are extremely important and explain a large number of problems of calculations with approximate functionals. When they are thought of separately, they can be tackled differently with hope of building better functionals. However we feel that the true understanding of the importance of fractional occupations comes when the two are considered at the same time and further extended [8].

We have considered separately H_2 and H_2^+, especially in the limit of infinite separation. In these cases, hydrogen atoms with fractional occupation numbers are obtained; in the fractional charge case $n_\alpha = \delta$ and $n_\beta = 0$, and in the fractional spin case $n_\alpha = \delta, n_\beta = (1 - \delta)$. These are two specific cases of fractional occupations that give rise to two very different perspectives on problems with functionals. Let us now consider the behaviour of all possible occupations for the hydrogen atom, $\mathrm{H}[n_\alpha, n_\beta]$, with $n_\alpha \leq 1$ and $n_\beta \leq 1$, i.e the hydrogen atom with up to two electrons going from H^+ to H^-.

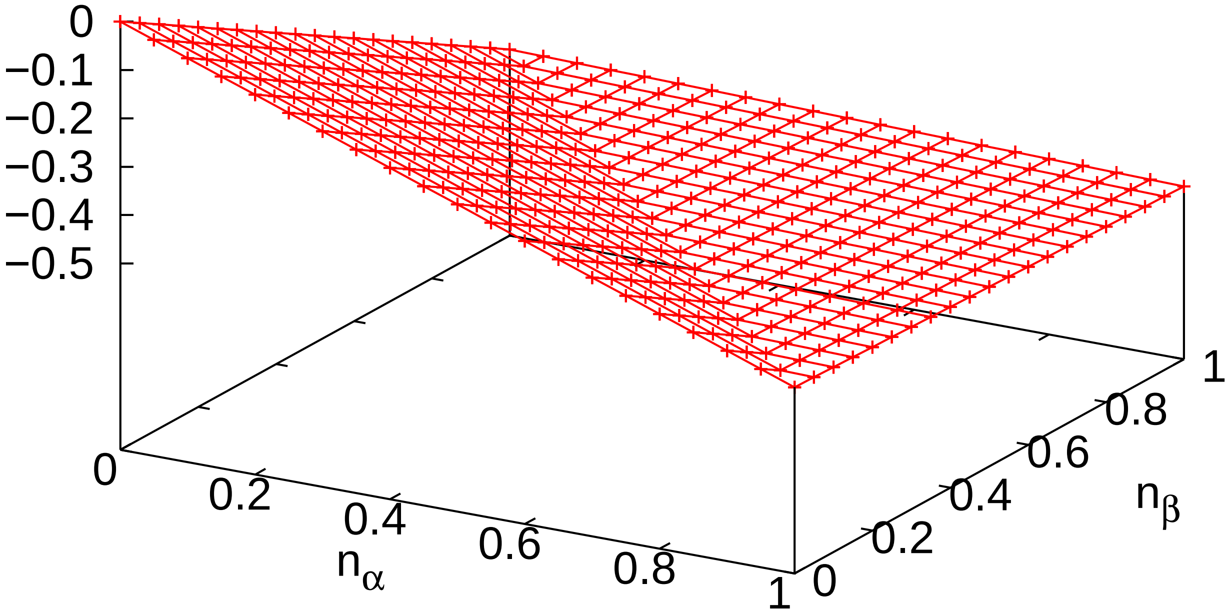

Figure 7: Flat-plane exact condition for the energy functional. It is a generalisation of the straight-line condition for fractional charges combined with the constancy condition for fractional spins. It is shown for the hydrogen atom with fractional occupations n_α and n_β.

The exact behaviour, derived in [8], is shown in Fig. 7 and is a generalisation of the PPLB result

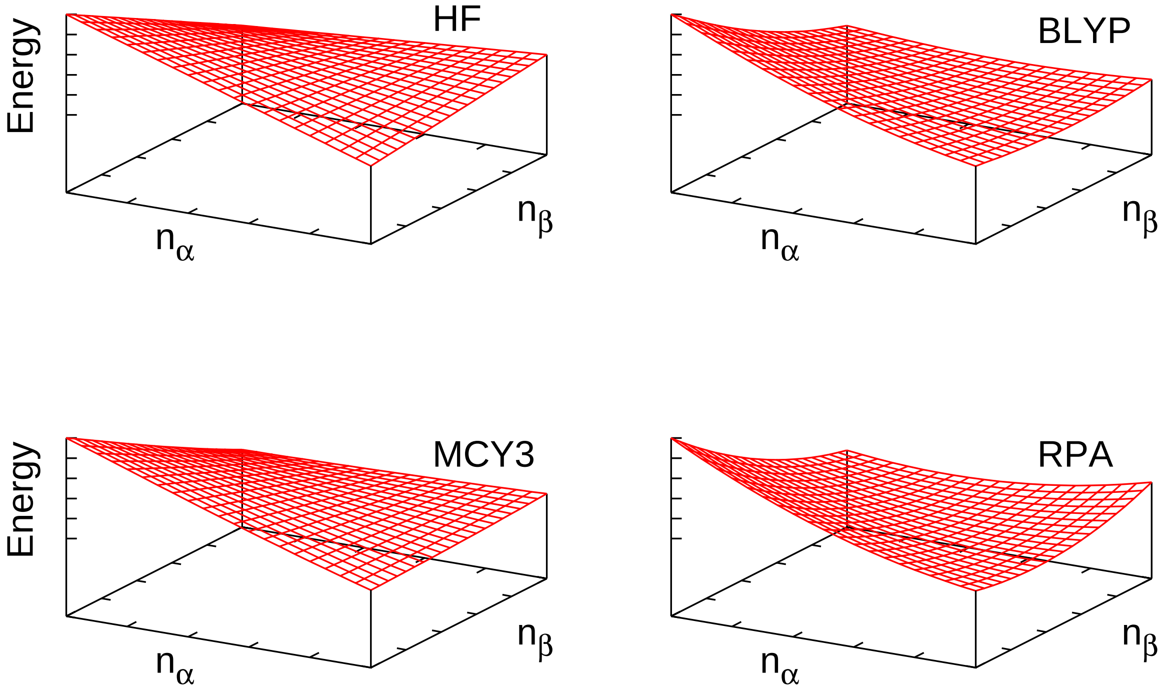

Figure 8: Testing different methods for the flat-plane conditions. All functional approximations in the literature as well as more sophisticated methods such as the random phase approximation (RPA) dramatically fail, missing the key discontinuty at integer number of electrons.

explicitly considering spin as well, as given by the constancy condition. The generalisation can be considered from the appropriate ensemble of the corner points from H[0,0], H[1,0], H[0,1] and H[1,1]. This 'flat-plane' behaviour may not be too surprising but the importance really comes from the consideration of currently used approximate functionals. Fig. 8 shows the behaviour of several representative exchange-correlation functionals, and all of them exhibit a striking qualitative failure to correctly describe the discontinuous behaviour of the exact energy. In practical terms this means that none of these methods (and extensions: mixing together, including range separation etc.) are able to describe $H[\frac{1}{2},0]$ and $H[\frac{1}{2},\frac{1}{2}]$ at the same time or, in terms of simple molecules, are unable to correctly describe the limit of stretched H_2^+ and stretched H_2 at the same time, or more generally, they cannot be both free from delocalisation error and static correlation error at the same time. Simple ideas will not work in this case, as an example, including more exact exchange in a functional decreases the delocalisation error but increases the static correlation error. Thus, the flat-plane condition clearly indicates that to get the energetics correct some sort of discontinuous behaviour, far from currently used forms, is needed in functionals.

5.7 Derivatives and the fundamental gap

From the consideration of the E vs N curve, there are two key expressions for the fundamental gap $(I - A)$, one from the difference of the energies at the integer points

$$E_{\text{gap}}^{\text{integer}} = [E(N-1) - E(N)] - [E(N) - E(N+1)] \tag{12}$$

and a second one from the initial derivatives at N to the left and the right

$$E_{\text{gap}}^{\text{deriv}} = \left.\frac{\partial E}{\partial N}\right|_{N-\delta} - \left.\frac{\partial E}{\partial N}\right|_{N+\delta}. \tag{13}$$

These two are equal for the exact functional due to the straight line behaviour in between the integers. However, interesting questions arise for approximate functionals:

1. How are the derivatives evaluated?
2. Is the functional a straight line in between the integers?
3. How are these derivatives connected to the Kohn-Sham eigenvalues?
4. What about the derivative discontinuity and Mott insulators?

To understand the derivatives we decide to differentiate with respect to the number of electrons, given the orbitals at N. This formally gives a derivation from potential functional theory [92, 93] that contrast with the classical way of Perdew-Levy [49] and Sham-Schlüter [50], where functional derivatives are taken with respect to the density. We feel this offers a useful way to understand and compute the derivatives related to the band-gap in DFT.

5.7.1 Evaluating the derivatives

We need to take the derivatives $\frac{\partial E}{\partial N}\big|_{N\pm\epsilon}$ for different functional approximations. If we consider the derivatives in $\{\phi_i, n_i\}$ space rather than the more conventional $\{\rho, N\}$ space, then they can be expressed slightly differently. The derivatives for energy expressions that have a smooth dependence on the density matrix are expressed in this space as [5]

$$\left.\frac{\partial E}{\partial N}\right|_{N-\epsilon} = \left(\frac{\partial E}{\partial n_{\text{homo}}}\right)_{\phi_i} \quad \text{and} \quad \left.\frac{\partial E}{\partial N}\right|_{N+\epsilon} = \left(\frac{\partial E}{\partial n_{\text{lumo}}}\right)_{\phi_i}. \tag{14}$$

Let us first consider the derivatives of the density taken in this manner where the orbitals are fixed

$$\left.\frac{\partial \rho(\mathbf{r})}{\partial N}\right|_{N\pm\epsilon} = \begin{cases} \phi_{\text{homo}}(\mathbf{r})\phi^*_{\text{homo}}(\mathbf{r}) & \text{for } N-\epsilon \\ \phi_{\text{lumo}}(\mathbf{r})\phi^*_{\text{lumo}}(\mathbf{r}) & \text{for } N+\epsilon. \end{cases} \tag{15}$$

This equation says that the density is discontinuous on passing through the integer and any term in calculating the derivatives that depends on the density will also have a discontinuity. For example, the derivative of the the fractional expression for the total energy, Eq. (8), using $E_x^{\text{LDA}} = -c_D \int \rho^{4/3}(\mathbf{r})\mathrm{d}\mathbf{r}$ for $E_{xc}[\rho]$, it is given by

$$\left.\frac{\partial E^{\text{LDA}}}{\partial N}\right|_{N-\epsilon} = \langle\phi_{\text{homo}}| - \frac{1}{2}\nabla^2 + v_{\text{ext}}(\mathbf{r}) + v_J(\mathbf{r}) - \frac{4}{3}c_D\rho^{1/3}(\mathbf{r})|\phi_{\text{homo}}\rangle, \tag{16}$$

and a very similar expression is obtained for $\frac{\partial E^{\mathrm{LDA}}}{\partial N}\Big|_{N+\epsilon}$ just with ϕ_{homo} replaced with ϕ_{lumo}. If we replace now $E_{xc}[\rho]$ by an orbital functional such as exact exchange, then the derivative to the left is given by

$$\frac{\partial E^{\mathrm{HF}}}{\partial N}\bigg|_{N-\epsilon} = \langle\phi_{\mathrm{homo}}| - \frac{1}{2}\nabla^2 + v_{\mathrm{ext}}(\mathbf{r}) + v_J(\mathbf{r}) - \sum_j \int \frac{\phi_j(\mathbf{r})\phi_j(\mathbf{r}')}{|\mathbf{r}-\mathbf{r}'|}\mathrm{d}\mathbf{r}' P_{\mathbf{r}\mathbf{r}'}|\phi_{\mathrm{homo}}\rangle, \tag{17}$$

and again the derivative to the right just given by replacing ϕ_{homo} by ϕ_{lumo}.

The gaps for both functionals can be expressed as [5]

$$E_{\mathrm{gap}} = \langle\phi_{\mathrm{lumo}}|H_{\mathrm{eff}}|\phi_{\mathrm{lumo}}\rangle - \langle\phi_{\mathrm{homo}}|H_{\mathrm{eff}}|\phi_{\mathrm{homo}}\rangle \tag{18}$$

where $H_{\mathrm{eff}}\phi_i = \frac{\partial E[\rho]}{\partial\phi_i(\mathbf{r})}$. For functionals of the density this is just the difference of the Kohn-Sham eigenvalues. For orbital functionals it is also the difference of the eigenvalues in a calculation which minimises the energy. In this case, not a pure Kohn-Sham type equation is solved because of the presence of orbital exchange type terms, and technically it is called generalised Kohn-Sham approach [10] or the Hartree-Fock Kohn-Sham method [2] . However, this is standard for most functionals of this type (e.g. a normal Hartree-Fock or B3LYP calculation). If a local potential is used for these type of functionals, as in an optimised effective potential (OEP) calculation [94–96], the Kohn-Sham eigenvalues obtained will not be the derivative of the energy because $\langle\phi_{\mathrm{f}}|H_s|\phi_{\mathrm{f}}\rangle \neq \langle\phi_{\mathrm{f}}|H_{\mathrm{eff}}|\phi_{\mathrm{f}}\rangle$.

For the exact exchange correlation functional

$$E_{\mathrm{gap}} = \langle\phi_{\mathrm{lumo}}|H_{\mathrm{eff}}|\phi_{\mathrm{lumo}}\rangle - \langle\phi_{\mathrm{homo}}|H_{\mathrm{eff}}|\phi_{\mathrm{homo}}\rangle + \mathcal{D}_{xc} \tag{19}$$

where $\mathcal{D}_{xc}$ covers any discontinuity beyond that of just changing orbitals, beyond smooth functionals [8].

5.7.2 Convexity, delocalisation error and the gap

Functionals such as LDA and GGA have a large amount of convex behaviour for finite systems. This gives a clear picture of the failure for their prediction of band-gaps from derivatives at N [6]. They clearly do not satisfy the linearity condition of the exact functional [38], and therefore the initial derivatives do not point to the integer points and henceforth do not give I and A. These derivatives for LDA and GGA are just the Kohn-Sham eigenvalues as $H_{\mathrm{eff}} = H_s$ in this case. The MCY3 functional was developed to minimise the delocalisation error in small systems [21]. For some atoms and molecules it was shown that it gives a good straight line behaviour and henceforth its derivatives [5] are accurate approximations to I and A.

The question of the non-linearity in the E vs N curve is maybe less directly key for larger systems, for which, as previously discussed in Fig. 4, the delocalisation error of functionals such as LDA or GGA means that an added electron will spread out too much and have much more linear behaviour. In Fig. 4, as the number of units increases the E vs N curve for a functional with delocalisation error gets straighter and straighter. There is therefore less disagreement between the $E_{\mathrm{gap}}^{\mathrm{deriv}}$ and $E_{\mathrm{gap}}^{\mathrm{integer}}$. In an ideal infinitely expanded solid a straight line is obtained with the wrong integer value at $N+1$, and therefore even though $E_{\mathrm{gap}}^{\mathrm{deriv}} = E_{\mathrm{gap}}^{\mathrm{integer}}$ they are both wrong. This explains the failure of LDA and GGA for the gap of semiconductors. Although MCY3 improves upon LDA for the gap of molecules, it does not help in solids because it uses long-range exact exchange. This ingredient is, however, key for fixing atoms and molecules but unfortunately massively overpredicts the gaps of most solids. Methods that are successful for the gap of solids are based on screening (e.g. GW [97]) which somehow removes the long-range part of exchange. The understanding from molecules can help in solids but, of course, different challenges for the exchange-correlation functional emerge when considering such different densities. There remains a critical challenge to develop functionals which can reliably predict, through the energy derivative with respect to the number of electrons, the energy gaps across the scales from atoms, molecules to bulks. Such a functional would be able to provide an accurate description of the electronic structure at interfaces, such as the alignment of the energy levels, and the amount and direction of charge transfer.

5.7.3 Kohn-Sham gaps and experimental band-gaps

Consider the exact Kohn-Sham expression for the derivative gap, as it is given by [49, 50]

$$\begin{aligned} E_{\text{gap}}^{\text{deriv}} &= \left(\left.\frac{\delta T_s}{\delta\rho(\mathbf{r})}\right|_{N-\delta} - \left.\frac{\delta T_s}{\delta\rho(\mathbf{r})}\right|_{N+\delta} \right) + \left(\left.\frac{\delta E_{xc}}{\delta\rho(\mathbf{r})}\right|_{N-\delta} - \left.\frac{\delta E_{xc}}{\delta\rho(\mathbf{r})}\right|_{N+\delta} \right) && (20) \\ &= \epsilon_{\text{lumo}}^{\text{KS}} - \epsilon_{\text{homo}}^{\text{KS}} + \Delta_{xc} && (21) \end{aligned}$$

This equation could be understood to state that even for an exact Kohn-Sham calculation giving the exact Kohn-Sham gap there is a missing derivative discontinuity term. In this understanding, a Kohn-Sham calculation with any approximate functional, up to and including the exact functional, does not give the experimental gap from its eigenvalues, an additional term is needed. This perspective, while correct, does not give information on how to understand and view the all important functional derivative discontinuity. To address this, it is appropriate to formulate the following question: given an explicit form for E_{xc}, what is the prediction of the gap? We can take these derivatives as above, giving

$$\begin{aligned} E_{\text{gap}}^{\text{deriv}} &= \left.\frac{\partial E}{\partial N}\right|_{N-\delta} - \left.\frac{\partial E}{\partial N}\right|_{N+\delta} && (22) \\ &= \langle \phi_{\text{lumo}} | H_{\text{eff}} | \phi_{\text{lumo}} \rangle - \langle \phi_{\text{homo}} | H_{\text{eff}} | \phi_{\text{homo}} \rangle + \mathcal{D}_{xc} && (23) \end{aligned}$$

For a functional such as LDA/GGA this gives just the difference of the Kohn-Sham eigenvalues, for an orbital functional such as Hartree-Fock this is not the difference of Kohn-Sham eigenvalues, it is the difference of generalised Kohn-Sham eigenvalues. The $\mathcal{D}_{xc}$ part just comes from the derivatives of the energy expression, however for any smooth functional of the orbitals or density $\mathcal{D}_{xc} = 0$. For derivatives of non-smooth functionals (e.g. Ref [8]) $\mathcal{D}_{xc} \neq 0$. Just to clarify, if we have the exact exchange-correlation functional the experimental gap does just come from taking the difference of the derivative to the left and the right. To get agreement with experiment we just need better approximate exchange-correlation functionals, with the correct discontinuous behaviour. It is important to understand that the derivative discontinuity is a question about the exchange-correlation functional not something beyond it.

5.7.4 Derivative discontinuity and Mott insulators

Mott Insulators are systems with a large experimental gap but from band structure calculations they look metallic (i.e they can have an odd number of electrons per unit cell or, in the language of molecules, a degenerate HOMO and LUMO). A simple example of a Mott insulator in the solid state is a transition metal oxide such as NiO. However, to better understand this issue from a DFT perspective, we can consider much simpler systems, either the infinitely stretched limit of H_2 or even more simply $H[\frac{1}{2}, \frac{1}{2}]$ [8]. If we first consider the case of infinitely stretched closed shell H_2, the usual gap as considered above comes from changing the orbital from the ϕ_{homo} to ϕ_{lumo}, however in this system both orbitals (σ_g and σ_u) are degenerate in energy and even have the same density. This means that any term that has a smooth dependence on the density (e.g. $J[\rho]$) or even any term that has a smooth dependence on the orbitals, such as $E_x^{\text{exact}}[\phi_i]$ or $T_s[\phi_i]$, will not contribute to the gap. For example the T_s term contribution to the gap

$$\langle\phi_{\text{lumo}}| - \frac{1}{2}\nabla^2|\phi_{\text{lumo}}\rangle - \langle\phi_{\text{homo}}| - \frac{1}{2}\nabla^2|\phi_{\text{homo}}\rangle = 0 \tag{24}$$

vanishes in this case due to the nature of the HOMO and LUMO. However the infinitely stretched system is just composed of two H atoms and therefore should have the same gap as a normal H atom, where the ionisation energy is 13.61 eV and the electron affinity is 0.75 eV, with a very large gap of 12.85 eV. All this gap must come from the exchange-correlation term.

Therefore for Mott insulators, all the contribution to the gap comes from the derivative discontinuity of the exchange correlation functional, with no contribution from the (generalised) Kohn-Sham eigenvalues:

$$E_{\text{gap}} = \left.\frac{\partial E_{xc}}{\partial N}\right|_{N-\delta} - \left.\frac{\partial E_{xc}}{\partial N}\right|_{N+\delta}. \tag{25}$$

For the gaps to be non-zero for Mott insulators, E_{xc} cannot be a continuous functional of either the density or the non-interacting density matrix [8].

5.8 Conclusions

Fractional charges and fractional spins, along with the corresponding exact constraints that characterise them, offer a unique view of density functional theory. Density functional approximations work well for systems with integer number of electrons (and character) but fail badly in systems that could be described as fractional. This failure can be easily seen from studying very simple systems, even those having one electron, leading to an intriguing and simple to understand view of the problems of functionals and the difficult paths to correct them. Radically new discontinuous behaviour is needed in the functional form to be able describe both H_2^+ and H_2 in their infinite limits or, more generally, to be free from delocalisation error and static correlation error at the same time. This discontinuous behaviour goes beyond that of orbital functionals and helps explain some key challenges of DFT in the literature, such as calculating band-gaps. The area of strong correlation is also related to this basic failure of current used exchange-correlation functionals to describe simultaneously fractional charges and spins. The hydrogen atom, although extremely simple and trivial to solve in quantum mechanics, highlights many key problems of DFT: delocalisation error, static correlation error, strong correlation and the derivative discontinuity.

5.9 Acknowledgements

We would like to dedicate this manuscript to the memory of Mr. Benjamin I. Cohen. The Royal Society, Ramón y Cajal and National Science Foundation are also acknowledged for financial support.

References

[1] P. Hohenberg, W. Kohn, Phys. Rev. B **136**, 864 (1964).

[2] R. G. Parr, W. Yang, *Density-Functional Theory of Atoms and Molecules* (Oxford University Press, New York, 1989).

[3] R. Dreizler, E. Gross, *Density-Functional Theory* (Springer-Verlag, Berlin, 1990).

[4] A. J. Cohen, P. Mori-Sánchez, W. Yang, Science **321**, 792 (2008).

[5] A. J. Cohen, P. Mori-Sánchez, W. Yang, Phys. Rev. B **77**, 115123 (2008).

[6] P. Mori-Sánchez, A. J. Cohen, W. Yang, Phys. Rev. Lett. **100**, 146401 (2008).

[7] A. J. Cohen, P. Mori-Sánchez, W. Yang, J. Chem. Phys. **129**, 121104 (2008).

[8] P. Mori-Sánchez, A. J. Cohen, W. Yang, Phys. Rev. Lett. **102**, 066403 (2009).

[9] W. Kohn, L. Sham, Phys. Rev. A **140**, 1133 (1965).

[10] A. Seidl, A. Görling, P. Vogl, J. A. Majewski, M. Levy, Phys. Rev. B **53**, 3764 (1996).

[11] A. D. Becke, J. Chem. Phys. **98**, 5648 (1993).

[12] C. Lee, W. Yang, R. G. Parr, Phys. Rev. B **37**, 785 (1988).

[13] C. Adamo, V. Barone, J. Chem. Phys. **110**, 6158 (1999).

[14] D. M. Bylander, L. Kleinman, Phys. Rev. B **41**, 7868 (1990).

[15] J. Heyd, G. E. Scuseria, M. Ernzerhof, J. Chem. Phys. **118**, 8207 (2003).

[16] A. Savin, *Recent Developments and Applications of Modern Density Functional Theory* (Elsevier, Amsterdam, Amsterdam, 1996), p. 327.

[17] P. M. W. Gill, Mol. Phys. **88**, 1005 (1996).

[18] H. Iikura, T. Tsuneda, T. Yanai, K. Hirao, J. Chem. Phys. **115**, 3540 (2001).

[19] J. W. Song, M. A. Watson, H. Sekino, K. Hirao, J. Chem. Phys. **129**, 024117 (2008).

[20] T. Yanai, D. P. Tew, N. C. Handy, Chem. Phys. Lett. **393**, 51 (2004).

[21] A. J. Cohen, P. Mori-Sánchez, W. Yang, J. Chem. Phys. **126**, 191109 (2007).

[22] R. Baer, D. Neuhauser, Phys. Rev. Lett. **94**, 043002 (2005).

[23] W. Yang, J. Chem. Phys. **109**, 10107 (1998).

[24] M. Seidl, J. P. Perdew, S. Kurth, Phys. Rev. Lett. **84**, 5070 (2000).

[25] P. Mori-Sánchez, A. J. Cohen, W. Yang, J. Chem. Phys. **124**, 091102 (2006).

[26] A. J. Cohen, P. Mori-Sanchez, W. Yang, J. Chem. Phys. **127**, 034101 (2007).

[27] A. M. Teale, S. Coriani, T. Helgaker, J. Chem. Phys. **132**, 164115 (2010).

[28] J. Jaramillo, M. Ernzerhof, G. E. Scuseria, J. Chem. Phys. **118**, 1068 (2003).

[29] A. D. Becke, J. Chem. Phys. **122**, 064101 (2005).

[30] H. Bahmann, A. Rodenberg, A. V. Arbuznikov, M. Kaupp, J. Chem. Phys. **126**, 011103 (2007).

[31] M. Kaupp, H. Bahmann, A. V. Arbuznikov, J. Chem. Phys. **127**, 194102 (2007).

[32] S. Grimme, J. Chem. Phys. **124**, 034108 (2006).

[33] J.-D. Chai, M. Head-Gordon, J. Chem. Phys. **128**, 084106 (2008).

[34] Y. Zhang, X. Xu, W. A. Goddard, Proc. Natl. Acad. Sci. **106**, 4963 (2009).

[35] F. Furche, J. Chem. Phys. **129**, 114105 (2008).

[36] J. Toulouse, I. C. Gerber, G. Jansen, A. Savin, J. G. Ángyán, Phys. Rev. Lett. **102**, 096404 (2009).

[37] B. G. Janesko, T. M. Henderson, G. E. Scuseria, J. Chem. Phys. **130**, 081105 (2009).

[38] J. P. Perdew, R. G. Parr, M. Levy, J. L. Balduz Jr., Phys. Rev. Lett. **49**, 1691 (1982).

[39] W. Yang, Y. Zhang, P. W. Ayers, Phys. Rev. Lett. **84**, 5172 (2000).

[40] J. F. Janak, Phys. Rev. B **18**, 7165 (1978).

[41] J. P. Perdew, *Density Functional Methods in Physics*, R. Dreizler, J. da Providencia, eds. (Plenum Press, NY, 1985), pp. 265–308.

[42] A. Ruzsinszky, J. P. Perdew, G. I. Csonka, O. A. Vydrov, G. E. Scuseria, J. Chem. Phys. **125**, 194112 (2006).

[43] P. Mori-Sánchez, A. J. Cohen, W. Yang, J. Chem. Phys. **125**, 201102 (2006).

[44] A. Ruzsinszky, J. P. Perdew, G. I. Csonka, O. A. Vydrov, G. E. Scuseria, J. Chem. Phys. **126**, 104102 (2006).

[45] A. D. Becke, J. Chem. Phys. **107**, 8554 (1997).

[46] Y. Zhao, D. Truhlar, J. Chem. Theory Comput. **1**, 415 (2005).

[47] Y. Zhao, N. Schultz, D. Truhlar, J. Chem. Theory Comput. **2**, 364 (2006).

[48] Y. Zhang, W. Yang, J. Chem. Phys. **109**, 2604 (1998).

[49] J. P. Perdew, M. Levy, Phys. Rev. Lett. **51**, 1884 (1983).

[50] L. J. Sham, M. Schlüter, Phys. Rev. Lett. **51**, 1888 (1983).

[51] E. J. Baerends, O. V. Gritsenko, J. Phys. Chem. A **101**, 5383 (1997).

[52] R. Stowasser, R. Hoffmann, J. Am. Chem. Soc. **121**, 3414 (1999).

[53] D. J. Tozer, N. C. Handy, J. Chem. Phys. **109**, 10180 (1998).

[54] M. Stadele, M. Moukara, J. A. Majewski, P. Vogl, A. Gorling, Phys. Rev. B **59**, 10031 (1999).

[55] S. Hamel, P. Duffy, M. E. Casida, D. R. Salahub, J. Electr. Spectr. and Relat. Phenom. **123**, 345 (2002).

[56] N. A. Lima, L. N. Oliveira, K. Capelle, Euro. Phys. Lett. **76**, 601 (2002).

[57] M. J. Allen, D. J. Tozer, Mol. Phys. **100**, 433 (2002).

[58] D. J. Tozer, J. Chem. Phys. **119**, 12697 (2003).

[59] M. Gruning, A. Marini, A. Rubio, Phys. Rev. B **74**, 161103(R) (2006).

[60] M. Gruning, A. Marini, A. Rubio, J. Chem. Phys. **124**, 154108 (2006).

[61] F. De Proft, N. Sablon, D. J. Tozer, P. Geerlings, Faraday Discuss. **135**, 151 (2007).

[62] S. Kummel, L. Kronik, Rev. Mod. Phys. **80**, 3 (2008).

[63] D. Vieira, K. Capelle, C. A. Ullrich, Phys. Chem. Chem. Phys. **11**, 4647 (2009).

[64] U. Salzner, R. Baer, J. Chem. Phys. **131**, 231101 (2009).

[65] P. Mori-Sánchez, A. J. Cohen, W. Yang (2009). http://arXiv.org/abs/0903.4403.

[66] W. Yang, P. Mori-Sánchez, A. J. Cohen (2010). In preparation.

[67] E. R. Johnson, *et al.*, J. Am. Chem. Soc. **132**, 6498 (2010).

[68] L. A. Curtiss, K. Raghavachari, P. C. Redfern, V. Rassolov, J. A. Pople, J. Chem. Phys. **109**, 7764 (1998).

[69] L. A. Curtiss, P. C. Redfern, K. Raghavachari, J. A. Pople, J. Chem. Phys. **114**, 108 (2001).

[70] B. G. Johnson, C. A. Gonzales, P. M. Gill, J. A. Pople, Chem. Phys. Lett. **221**, 100 (1994).

[71] Y. Zhao, B. J. Lynch, D. G. Truhlar, J. Phys. Chem. A **108**, 2715 (2004).

[72] J. Zheng, Y. Zhao, D. G. Truhlar, J. Chem. Theory Comput. **3**, 569 (2007).

[73] Y. Zhao, D. G. Truhlar, Org. Lett. **8**, 5753 (2006).

[74] M. D. Wodrich, *et al.*, Chem. Eur. J. **13**, 7731 (2007).

[75] S. E. Wheeler, K. N. Houk, P. V. R. Schleyer, W. D. Allen, J. Am. Chem. Soc. **131**, 2547 (2009).

[76] S. E. Wheeler, A. Moran, S. N. Pieniazek, K. N. Houk, J. Phys. Chem. A **113**, 10376 (2009).

[77] M. Korth, S. Grimme, J. Chem. Theory Comput. **5**, 993 (2009).

[78] K. Raghavachari, *et al.*, Chem. Phys. Lett. **214**, 357 (1993).

[79] C. Castro, W. L. Karney, C. M. McShane, R. P. Pemberton, J. Org. Chem **71**, 3001 (2006).

[80] R. A. King, T. D. Crawford, J. F. Stanton, H. F. Schaefer, J. Am. Chem. Soc. **121**, 10788 (1999).

[81] T. Heaton-Burgess, W. Yang, J. Chem. Phys. (2010). In Press.

[82] E. R. Johnson, P. Mori-Sanchez, A. J. Cohen, W. Yang, J. Chem. Phys. **129**, 204112 (2008).

[83] G. I. Csonka, A. Ruzsinszky, J. P. Perdew, S. Grimme, J. Chem. Theory Comput. **4**, 888 (2008).

[84] A. Savin, Chem. Phys. **356**, 91 (2009).

[85] P. Gori-Giorgi, A. Savin, J. Phys. Conf. Ser. **117**, 12017 (2008).

[86] E. J. Baerends, Phys. Rev. Lett. **87**, 133004 (2001).

[87] M. Fuchs, Y. M. Niquet, X. Gonze, K. Burke, J. Chem. Phys. **122**, 094116 (2005).

[88] M. J. G. Peach, A. M. Teale, D. J. Tozer, J. Chem. Phys. **126**, 244104 (2007).

[89] K. Andersson, P.-A. Malmqvist, B. O. Roos, J. Chem. Phys. **96**, 1218 (1992).

[90] J. Grafenstein, D. Cremer, Phys. Chem. Chem. Phys. **2**, 2091 (2000).

[91] J. Grafenstein, D. Cremer, Mol. Phys. **103**, 279 (2005).

[92] W. Yang, P. W. Ayers, Q. Wu, Phys. Rev. Lett. **92**, 146404 (2004).

[93] A. J. Cohen, P. Mori-Sánchez, W. Yang, J. Chem. Theory Comput. **5**, 786 (2009).

[94] R. T. Sharp, G. Horton, Phys. Rev. **90**, 317 (1953).

[95] J. D. Talman, W. F. Shadwick, Phys. Rev. A **14**, 36 (1976).

[96] W. Yang, Q. Wu, Phys. Rev. Lett. **89**, 143002/1 (2002).

[97] G. Onida, L. Reining, A. Rubio, Rev. Mod. Phys. **74**, 601 (2002).